Univerzita Karlova
Přírodovědecká fakulta

Studijní program: Biologie
Studijní obor: Fyziologie živočichů

Bc. Petra Suchá

Úloha spojovacích proteinů při stabilizaci extracelulární matrix v mozku a při vytváření a udržování perineurálních sítí

The role of link proteins in the stabilization of the brain extracellular matrix and in formation and maintaining of the perineuronal nets

Diplomová práce

Vedoucí diplomové práce: doc. MUDr. Lýdia Vargová, Ph.D.

Praha, 2017

Prohlášení:

Prohlašuji, že jsem diplomovou práci zpracovala samostatně a že jsem uvedla všechny použité informační zdroje a literaturu. Tato práce ani její podstatná část nebyla předložena k získání jiného nebo stejného akademického titulu.

V Praze, dne 1. května 2017

Petra Suchá

Poděkování

Ráda bych poděkovala vedoucí své diplomové práce doc. MUDr. Lýdii Vargové, Ph.D. za ochotu, trpělivost a cenné rady, které mi při vypracování diplomové práce pomohly. Dále bych ráda poděkovala svým kolegům Mgr. Marcelovi Bochinovi, RNDr. Martině Chmelové Ph.D. a Bc. Monice Kamenické z laboratoře difúzních měření Ústavu Neurověd 2. lékařské fakulty Univerzity Karlovy, kteří participovali na experimentech a vytvořili dobrou pracovní atmosféru.

Abstrakt

Extracelulární prostor vyplňují specifické makromolekuly vytvářející extracelulární matrix, která díky obsaženým negativním nábojům může ovlivňovat difuzi vody, iontů a molekul. V určitých oblastech mozku, vytváří molekuly extracelulární matrix komplexní, síťovitou struktury tzv. perineurální sítě, které se poprvé objevují s koncem kritické periody, stabilizují synapse a snižují synaptickou plasticitu. Úlohu Bral2 proteinu v stabilizaci perineurálních sítí jsme studovali pomocí měření difuzních parametrů iontoforetickou TMA^+ metodou v reálném čase a pomocí imunohistochemické analýzy GFAP pozitivních buněk a kvantifikace exprese specifických molekul extracelulární matrix u kontrol a Bral2 deficientních myší. Dále byly porovnány změny vzniklé delecí spojovacího proteinu Bral2 se změnami, které nastaly po enzymatickém natrávení extracelulární matrix. U Bral2 deficientních myší jsme ve srovnání s kontrolou nalezli signifikantní snížení tortuosity v jádře trapézovitého tělesa. Tato změna se projevuje až v důsledku stárnutí a u mladých myší nebyla prokázána. Imunohistochemická analýza ukázala, že inferior colliculus neobsahuje perineurální sítě založené na Bral2 a brevikanu a použili jsme ho proto jako negativní kontrolu. V obou jádrech však byli viditelné perineurální sítě založené na Crtl1 a agrekanu. Brevikan, který je obyčejně exprimován společně s Bral2, měl u Bral2 deficitních myší zachovalou expresi vázanou na perineurální sítě, což naznačuje reorganizaci extracelulární matrix a nahrazení Bral2 jiným spojovacím proteinem. Naše výsledky naznačují, že vliv stárnutí na demaskování účinku deficitu Bral2 na extracelulární difúzi je pravděpodobně nepřímý a může být spojen s nedostatečným neuroprotektivním účinkem a tudíž vyšší senzitivitou ke změnám, vyvolaným stárnutím a to včetně morfologické přestavby astrocytů. Na rozdíl od deficitu Bral2 spojovacího proteinu, vedla aplikace chondroitinázy ke zvýšení tortuosity, nejspíše kvůli přítomnosti naštěpených, ale stále přítomných molekul extracelulární matrix, které vyplnily extracelulární prostor, a ztížili difúzi. Rozdíly mezi našimi a předchozími nálezy však naznačují, že účinek enzymatického natrávení může záviset na struktuře tkáně a může se v jednotlivých oblastech lišit.

Klíčová slova: extracelulární prostor, extracelulární matrix, perineurální sítě, spojovací protein, difúzní parametry

Abstract

The brain extracellular space (ECS) contains specified macromolecules forming the extracellular matrix (ECM), containing a high amount of negative charges that could bind water or other soluble ions and molecules diffusing within the ECS. In specific brain areas, the ECM molecules form a condensed, reticular-like structure of perineuronal nets (PNNs). It has been found that PNNs appear at the end of the critical period, when they stabilize the synapses and terminate their plasticity and may have also neuroprotective function. To study the role of brain link protein 2 (Bral2) in stabilizing the ECM complexes, we employed the real-time iontophoretic method and immunohistochemical analysis to show the difference in the ECS diffusion parameters and level of expression of the ECM molecules between the wild type and Bral2-deficient mice. We also compared changes in the ECS diffusion parameters induced by Bral2 deficiency with those appeared after enzymatic destruction of the ECM by the chondroitinase ABC (chABC). In the Bral2-deficient mice, we discovered significantly decreased values of tortuosity in the trapezoid body. This difference was age related and did not manifest itself in young mice. Immunohistochemical analysis showed that inferior colliculus does not contain Bral2-brevican based perineuronal nets. Therefore, we used inferior colliculus as a negative control. On the other hand, the Crtl1-aggrecan-based perineuronal nets were present in the both studied nuclei. Brevican, which usually co-localize with Bral2, maintained the PNN-like pattern in the trapezoid body of the Bral2-deficient mice, indicating the reorganization of the ECM and substitution of Bral2 by another link protein. Our results suggest that the effect of aging on disclosure of the Bral2 deficiency-evoked changes in the extracellular diffusion is probably indirect. This effect may be related to the insufficient neuroprotection and so higher sensitivity to aging-related changes, including morphological transformation of GFAP positive cells. Unlike Bral2 deficiency, application of the chABC resulted in an increase in tortuosity, probably caused by a raised level of enzymatically cleaved molecules that were still present in the ECS and hindered the diffusion. The difference between our results and previous finding in the literature suggests that the efficacy of the enzymatic cleavage can depend on the tissue structure and thus, it can vary in the different regions.

Keywords: extracellular space, extracellular matrix, perineuronal nets, link protein, diffusion parameters

Table of contents

List of abbreviations

aCSF – artificial cerebrospinal fluid

AD – Alzheimer's disease

ADC_W – apparent diffusion coefficient of water

AMPA – α-amino-3-hydroxy-5-methyl-4-isoxazolepropionic acid

CNS – central nervous system

CSPG – chondroitin sulfate proteoglycan

DAPI – 4', 6-diamidino-2-phenylindole

DCN – deep cerebellar nuclei

DW-MRI – diffusion weighted magnetic resonance imaging

ECS – extracellular space

ECM – extracellular matrix

GABA – γ-aminobutyric acid

GFAP – glial fibrillary acidic protein

HA – hyaluronic acid

HAPLN – hyaluronan and proteoglycan binding link protein

Has – hyaluronic acid synthase

chABC – chondroitinase ABC

IC – inferior colliculus

IOI – integrative optical imaging

ISM – ion-selective microelectrode

KO – knockout

LP – link protein

LTD – long-term depression

LTP – long-term potentiation

MMP – matrix metalloproteinase

NG2 – chondroitin sulfate proteoglycan NG2

NMDA – N-methyl D-aspartate

NMDG – N-methyl-D-glucamine

P – postnatal day

PBS – phosphate-buffered saline

PKC – proteinkinase C

PNN – perineuronal net

PV - parvalbumin

TB – medial nucleus of the trapezoid body

TMA – tetramethylammonium

TN – tenascin

TNF – tumor necrosis factor

TTX – tetrodotoxin

SEM – standard error of the mean

WFA – *Wisteria floribunda* agglutinin

WT – wild type

1. Introduction

The brain contains neurons, responsible for signal transmission, and of glial cells, which are not any less important for proper information transfer due to their homeostatic control mechanisms or myelin production. Moreover, glial cells themselves could modulate the signal transmission via calcium signaling and transmitter release (Perea and Araque 2005). Proper function of each neuron is very dependent on microenvironment formed by the surrounding extracellular space (ECS). The ECS in the central nervous system (CNS) is filled with interstitial fluid containing ions, molecules of neurotransmitters, trophic factors, hormones, and last but not least it is filled with extracellular matrix (ECM) molecules, which provide a structural support for nervous cells and are involved in cell migration, differentiation, synaptogenesis and synaptic plasticity (Dityatev and Schachner 2006). Around certain populations of neurons, ECM molecules form a dense and organized structure of the perineuronal nets (PNNs) (Deepa et al. 2006), which play an important role in synaptic plasticity and neuronal protection (Pizzorusso et al. 2002; Cabungcal et al. 2013). Link proteins (LP) that stabilize the bond between hyaluronic acid (HA) and proteoglycans in the PNNs (Melching and Roughley 1985) are highly studied in connection with their importance for the maintenance of the PNN structure.

The PNNs were firstly observed by Camillo Golgi and Santiago Ramon y Cajal in the 1890s as a reticular network on the neuronal surface and till now, the existence of PNNs has been shown in many species. In mammals, for example in mice (Murakami, Ohtsuka, and Ono 1996), rat (Brückner et al. 1994; Galtrey et al. 2008), human (Bertolotto et al. 1991; Murakami, Taguchi, and Ohtsuka 1993), monkey (Hendry et al. 1988; Adams et al. 2001) or in birds such as *Gallus domesticus* (Morawski et al. 2009). There is also an evidence for the appearance of PNN-like structures in invertebrates (Treherne, Schofield, and Lane 1982). PNNs are most numerous in primary motor, auditory and visual cortices (Bertolotto et al. 1991; Brückner et al. 1999; Hilbig et al. 2007; Galtrey et al. 2008) through the vertebrate group.

2. Extracellular space and extracellular matrix

The ECS occupies a considerable part, about 20 %, of the whole brain tissue (C. Nicholson and Syková 1998). From *in vivo* diffusion analysis with dextrans is believed that ECS width could be more than 35 nm in diameter (dextran with that width, could diffuse within ECS) (Thorne and Nicholson 2006). ECS is not a simple interstitial liquid with diluted ions and molecules. Under the control of the external signals, brain cells secrete macromolecules as collagen, elastin, glycoproteins (fibronectin, laminin, and tenascin), proteoglycans and hyaluronic acid. However, the fibrillar proteins as collagens and elastin are located only in particular sites in the CNS as in blood vessels or meninges and are usually excluded from the brain tissue (Shellswell et al. 1979). The remaining macromolecules are involved in the ECM and provide more than just a structural function as they are also important, for example, in the brain development and learning. The ECM influences the cell migration, maturation and differentiation depending on its composition and its ability to bind secreted molecules (like growth factors) and ions (Taipale and Keski-Oja 1997; Dityatev and Schachner 2006). It plays role in synaptic plasticity and synaptogenesis and supports maintaining of ion homeostasis (Galtrey and Fawcett 2007; Theocharis et al. 2015) by hindering the diffusion of ions and molecules within the ECS due to its charge (Hrabetová et al. 2009).

The cell to cell communication on the synaptic level is dependent on diffusion of substances through the synaptic cleft. The model of the tripartite synapse refers to a concept of synapse, where pre and postsynaptic neuron is complemented with the astrocytic processes, which enwrap the synapse and modulate the synaptic transmission (Araque et al. 1999). Even though synaptic transmission between individual neurons is considered to be the most important and well-studied way for information transfer, neurons may communicate with other neurons and glial cells also by an extra-synaptic “volume” transmission, which is mediated via the diffusion of neuroactive substances within the ECS (Zoli et al. 1999; Agnati et al. 2006; Vargová and Syková 2014). Volume transmission is important for communication between independent synapses (synaptic cross-talk), which could result in modulation of the final output. When the synapse is “open” (loosely ensheathed by glia and the ECM), the neurotransmitter could escape the cleft and diffuse away from its release site and affect the neighboring neurons via its interaction with the high-affinity receptors. Such influence is important for a long-term potentiation or depression (LTP or LTD) or during lactation, where

the tissue remodeling and changes in the ECS diffusion potentiate hormone release (Asztely, Erdemli, and Kullmann 1997; Piet et al. 2004).

For its role at the synaptic transmission, the ECM is often considered to be a fourth element added to the "tripartite synapse" model consisting of presynaptic, postsynaptic neuron and astrocytic endfeet (Dityatev and Rusakov 2011). ECM is also a potent creator of diffusion barriers in ECS and may thus influence both the extrasynaptic as well as the synaptic transmission (Vargová and Syková 2008).

2.1 ECS diffusion parameters

The ECS can be fairly accurately described by the ECS diffusion parameters. The ECS volume fraction α represents the space of the brain, where molecules could diffuse with exclusion of the intracellular space and it is defined as the ECS volume divided by a volume of the whole brain tissue (Fig. 1).

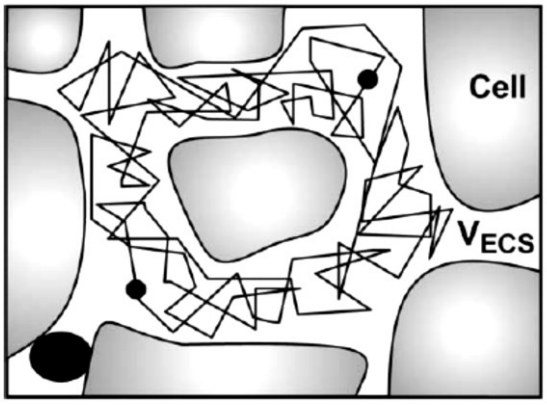

Figure 1: Volume fraction. Extracellular space available for diffusing molecule. Taken from (Vargová and Syková 2014)**.**

Tortuosity defines the ability of the environment to hinder the diffusion of ions and molecules of various weights and charges. The tortuosity is defined as a second root of the ratio of a diffusion coefficient measured in free medium ($cm^2.s^{-1}$), such as water or diluted gel, and an effective diffusion coefficient measured experimentally in the brain. It is dimensionless parameter and its usual value for ions or small molecules is around 1.5 in the brain. That means that the velocity of diffusion from a point A to a point B is about 2.5 times slower than in the

free medium. However, molecules of higher weight could be hindered more, because of the finite space between the cells. The origin of the hindrance, that diffusing molecules experience, lies on the basis of many factors. One of the factors that determine diffusion time of the molecule is length of a geometric path. This is a theoretical pathway, which the molecule has to follow and which is dependent on the size of the cells, their contours and processes. The other factor is an extension to the previous parameter and it is characterized as so called dead-space microdomains (Fig. 2). You can imagine it like dead-end invaginations of the cells or bigger space between the cells (as it is on the contact of edges of neighboring cells) or it could be the space between individual layers of myelin sheaths. Other important factors that hinder the molecules are the ECM molecules, which could affect the diffusion depending on their amount and charge and cellular (especially glial) processes forming diffusion barriers.

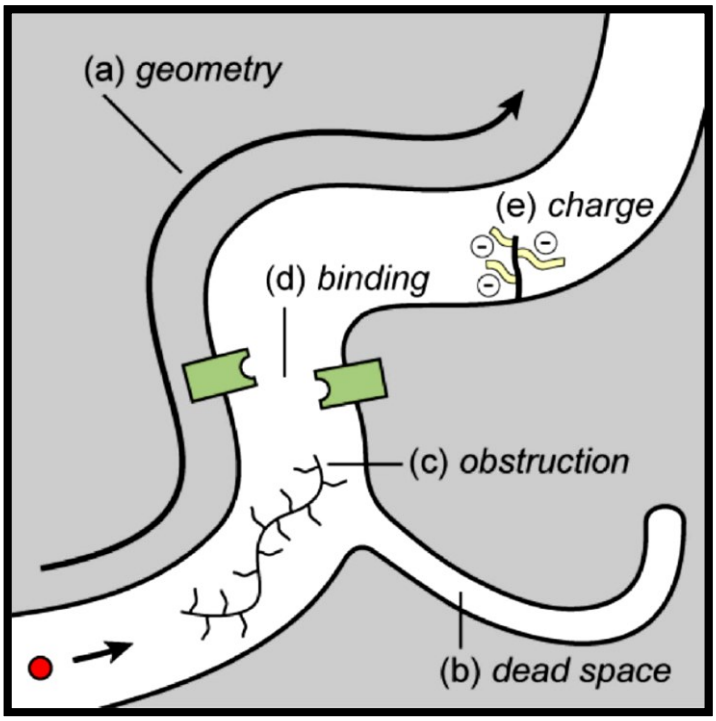

Figure 2: Factors affecting the diffusion. It is: a) geometry of the ECS determining the path the molecule will travel, b) dead-space microdomain is local enlargement of the ECS or invagination, where the molecule is trapped for some time, c) obstruction in form of the ECM molecules, d) binding sites for the molecule either on the cell membrane (receptor) or ECM, e) fixed negative charge of the ECM (affect the diffusion on charged molecules). Taken from (Syková and Nicholson 2008).

In certain brain regions, we can observe so called diffusion anisotropy (Voříšek and Syková 1997a; Prokopová, Vargová, and Syková 1997). It manifests itself as different values of tortuosity along different axes. The anisotropy can be detected usually in the myelinated white matter in relation to the orientation of the myelinated axon fibers. In agreement with this statement is the fact that anisotropy in the white matter increases during development in the same time course when the myelination occurs (Prokopová, Vargová, and Syková 1997; Voříšek and Syková 1997a; Chvátal et al. 1997). However, anisotropic diffusion can be found also in a subcortical grey matter, usually in the areas with a distinct organization of the fine astrocytic processes (Mazel, Simonová, and Syková 1998; Syková et al. 1998)

When measuring the diffusion of ions and molecules within the brain, it is also important to take into account the uptake of the diffusing substance into cells, across the blood-brain barrier and into the blood vessels. This uptake could be non-specific and concentration-dependent or it could be a specific transport via energy-dependent membrane transporter (as for glutamate) and could be reversible or irreversible (Ch. Nicholson 1992).

The values of tortuosity and volume fraction are not unchangeable, but they vary within physiological and pathophysiological states. Quantitative and/or qualitative changes in the ECM expression are often associated with the ECS diffusion parameter changes, as it can affect both volume fraction (high water contents makes the ECM almost incompressible so its increased content increases the ECS volume and vice versa) as well as tortuosity (ECM creates diffusion barriers). Transmembrane ion fluxes during neuronal activity induce movement of water causing cellular swelling followed by the RCS volume fraction decrease and tortuosity increase (Svoboda and Syková 1991). Additionally, the ECS volume fraction diminish with age and is largest in the newborn rats (Lehmenkühler et al. 1993; Syková et al. 2002). Aging is a physiological condition associated with decreased number and efficacy of synapses, neuronal loss, hyperplasia or hypertrophy of glial fibrillary acidic protein (GFAP) positive astrocytes (Syková, Mazel, and Šimonová 1998; Syková et al. 2002), demyelination, deposits of β-amyloid and changes in the ECM proteins resembling pathological states. Aging of brain usually results in change of the ECS diffusion parameters. The ECS volume fraction is often decreased and tortuosity increased in aged animals (Syková, Mazel, and Šimonová 1998). These alterations could be caused by changes that are mentioned previously in this paragraph.

Even more pronounced are these changes during pathological events. For example, during cell swelling in studies, where the experiments included changes in osmolality of the ECS, there is an inversely proportional relation observed as the decrease in the ECS volume fraction and increase in tortuosity during hypo-osmotic challenge (Kume-Kick et al. 2002; K. C. Chen and Nicholson 2000). This is similar with changes in anoxia, hypoxia or ischemia (Syková et al. 1994; Lundbaek and Hansen 1992; Vořišek and Syková 1997b). In states resulting in the overexpression of the ECM molecules as in tissue primary brain tumor (Zámečník et al. 2004) or in the focal cortical dysplasia (Zámečník et al. 2012), there is an increase in the ECS volume fraction and tortuosity. Long-lasting changes in post-traumatic states associated with cell death, astrogliosis and the ECM production are characterized by an enlargement of the ECS volume fraction and higher tortuosity values (Vořišek et al. 2002; Roitbak and Syková 1999). In knockout animals for a certain ECM molecules, like tenascin-R (TN-R) or brain link protein 1 (Bral1) there is a significant decrease in the ECS volume fraction and tortuosity (Syková et al. 2005) or tortuosity alone (Bekku et al. 2010).

2.2 Methods used for diffusion measurements

There were many methods to this date, which were used to determine diffusion parameters in the brain like measurements of tissue resistance (Van Harreveld, Dafny, and Khattab 1971), radiotracer method (Fenstermacher and Kaye 1988), changes in light transmittance and/or scattering (IOS method) (Fayuk et al. 2002; Syková et al. 2003), optical imaging with fluorescent dye (IOI) (C. Nicholson and Tao 1993), diffusion-weighted magnetic resonance (Sotak 2004) and real-time iontophoretic method (Lux and Neher 1973). The real-time iontophoretic method is the only one that determines the absolute values of all three ECS diffusion parameters concomitantly in living tissue slices and also *in vivo*. This method is based on measurements of time-dependent changes of concentration of tetramethylammonium ion (TMA^+) with ion-selective microelectrode (C. Nicholson and Phillips 1981). Other mentioned methods are able to measure either one diffusion parameter or only a relative change in the ECS volume fraction. However, some methods could be still advantageous in certain studies. The IOI method could be used with wide range of molecules, where is the possibility to attach the fluorescent dye and it is able also to register the diffusion anisotropy in real-time (Xiao et al. 2008). Diffusion-weighted magnetic resonance (DW-MRI),

as a non-invasive method could be employed in animal and patient studies to determine apparent diffusion coefficient of water (ADC_W). However, as water permeates cell membrane, so DW-MRI measures rate of both extracellular and intracellular water diffusion (Sotak 2004).

3. Extracellular matrix and perineuronal nets

ECM is a collection of secreted molecules providing structural and biochemical support in the ECS. The ECM consists of macromolecules that could be divided into the three major groups: a) glycosaminoglycans (hyaluronic acid); b) proteoglycans; and c) glycoproteins. The function of ECM molecules is complex and includes e.g. role in migration, proliferation and differentiation of stem cells, axonal growth, synapse formation and synaptic plasticity, responses to changes caused by for example trauma or ageing and formation of condensed neuroprotective nets surrounding neurons and synapses - perineuronal nets (PNNs) and axonal coats (AC) (Dityatev and Fellin 2008).

3.1 ECM molecules

3.1.1 Proteoglycans, Hyaluronan and Tenascins

Proteoglycans are composed of core protein with covalently bound glycosaminoglycan chains (Fig. 3). There are many types of proteoglycans depending on the gene encoding the core protein, its splice variant and type and number of glycosaminoglycan chains. The proteoglycans present in complex extracellular matrix structures (perineuronal and perinodal matrix or AC) are neurocan, versican, brevican, aggrecan and phosphacan. Neurocan, brevican and versican V2 are mainly components of perinodal matrix in the white matter (Bekku et al. 2009; Bekku and Oohashi 2010). Aggrecan is a component of PNNs around soma, proximal dendrite and initial segment as is the brevican in some cases (Galtrey et al. 2008). Phosphacan is present in both grey (perineuronal nets) and white matter (perinodal nets). It is an extracellular variant of receptor-type tyrosine phosphatase (RPTPζ/β) (Galtrey et al. 2008; Maurel et al. 1994).

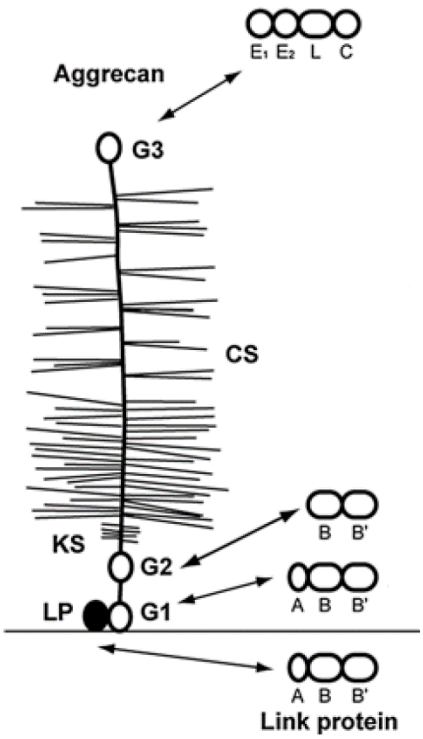

Figure 3: Structure of lectican aggrecan and link protein. Lecticans are bound to HA through their G1 domain at the N-terminal and this bond is stabilized by link proteins with the structure same as the G1 domain of lecticans. G1 domain contains Ig-like repeat (A) and proteoglycan tandem repeats (B, B'), which are also found in G2 domain. G3 domain at C-terminal consists of EGF-like repeats (E_1, E_2), a C-type lectin repeat (L) and complement regulatory protein-like repeat (C). The central region is a protein and different number of bound chondroitin sulfate (CS) and possibly keratin sulfate (KS) chains. LP - link protein; KS – keratin sulfate; CS – chondroitin sulfate; Ig – immunoglobulin; EGF – epidermal growth factor. Taken from (Aspberg 2016).

Hyaluronic acid composed of N-acetylglucosamin and D-glucuronic acid disaccharide units forms a backbone for other components. It has a polymeric structure synthetized by 3 isoforms of one enzyme called HA synthase (Has), which could be found inside the membrane and which is also considered the main structure for binding PNNs (through HA) to the membrane (Carulli et al. 2006; Arranz et al. 2014).

Tenascins are large ECM glycoproteins with five known isoforms (Jones and Jones 2000) with two of them participating in PNNs formation: TN-R and TN-C (Weber et al. 1999).

They are commonly seen as dimers or trimers, in case of TN-R, and hexamers in case of TN-C.

Different components of PNNs could be expressed by neurons or glial cells or by both. Neurons are mainly source of neurocan, aggrecan, TN-R, brevican and phosphacan. Brevican is also produced by astrocytes. NG2-possitive cells express versican V2, phosphacan and TN-R and oligodendrocytes versican V2 and TN-R. These data were obtained in the rat cerebellum (Carulli et al. 2006), but this pattern is similar in other areas (Galtrey et al. 2008).

3.1.2 Link proteins

The first known link protein (LP) was cartilage link protein 1 (Crtl1) originally observed in a cartilage. Later, more cartilage-like LPs were discovered in CNS (Asher et al. 1995). Their role is to stabilize the bond between HA and CSPGs of lectican family (Hardingham 1979; Melching and Roughley 1985). Four known LPs belong to one gene family - hyaluronan and proteoglycan binding link protein *gene family* (HAPLN). The members of HAPLN family are - HAPLN1 (Crtl1), HAPLN2 (Bral1) and HAPLN3 and HAPLN4 (Bral2) (Spicer, Joo, and Bowling 2003). The similarity between LPs is around 50% and human and mouse HAPLN proteins share above 80% identity. The LPs co-localize with CSPGs core protein gene on the chromosomes – HAPLN2 with brevican, HAPLN1 with versican, HAPLN3 with aggrecan, HAPLN4 with neurocan (Spicer, Joo, and Bowling 2003). HAPLN2 and 4 are restricted only to the brain and CNS (Spicer, Joo, and Bowling 2003) and it is interesting that those two LP often co-localize with particular CSPGs. Bral1 is co-localized with versican V2 isoform at the nodes of Ranvier in mouse white matter and it is important for conduction velocity in axons (Oohashi et al. 2002; Bekku et al. 2010). Bral2 LP is the most abundant in cerebellum and brainstem and often co-localizes with brevican (Bekku et al. 2003). Expression of Bral2 protein mRNA starts around P20 in neurons (Bekku et al. 2003). While Crtl1 is the most ubiquitous LP in the CNS and important for development of the PNNs (Carulli et al. 2010), the Bral2 is restricted to vestibulo-cochlear system, deep cerebellar nuclei, brainstem nuclei and ventral posteromedial and posterolateral thalamic nuclei (Bekku et al. 2003).

3.2 Perineuronal nets

PNNs are a product of higher organization of ECM molecules (Fig. 4). The main backbone forms the hyaluronic acid (HA) with sites that bind proteoglycans, which are furthermore cross-linked by tenascin molecules. Chondroitin sulfate proteoglycans (CSPGs) of lectican family – aggrecan, neurocan, versican, brevican - or phosphacan (Hagihara et al. 1999; Deepa et al. 2006) are linked to HA by their N-terminal domains and this covalent bond is stabilized by LPs. On the C-terminal domain of CSPGs is a binding motif for tenascin (Celio and Chiquet-Ehrismann 1993) dimers or trimers (early in development hexamers) that are cross-linking the CSPGs and thus contribute to condensed form of PNNs (Galtrey et al. 2008; Aspberg et al. 1997; Lundell et al. 2004). In was shown that hyaluronan, TN-R and many CSPGs are ubiquitous through the brain while aggrecan and link proteins are exceptional to PNNs (Galtrey et al. 2008).

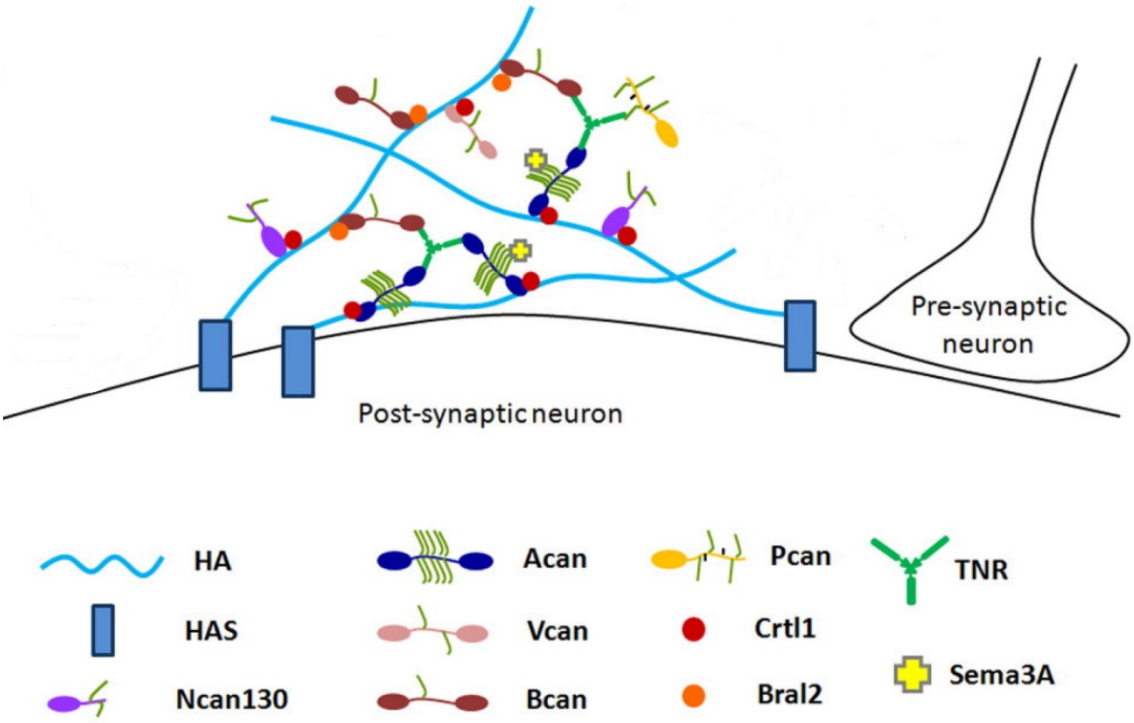

Figure 4: A schematic structure of PNNs. Hyaluronan (HA) is bound to the membrane by hyaluronan synthase (Has) and form a backbone for binding of CSPGs. The bond between CSPGs and HA is stabilized with link proteins. This whole net is cross-linked by tenascins. On the picture is presented the assumption that particular link protein is associated with particular CSPG. There is also shown the binding of semaphorin3A (see chapter 3.2.3). Taken from (Oohashi et al. 2015).

3.2.1 PNNs bearing neurons

PNNs are expressed in many areas of the brain. The most prominent and studied are the PNNs in the primary sensory and motor cortices, hippocampus, red nucleus, medial nucleus of the trapezoid body (TB), reticular thalamic nucleus, ventropostero medial thalamic nucleus, deep cerebellar nuclei, inferior colliculus (IC) or subtantia nigra (Brückner et al. 2000; Bertolotto, Manzardo, and Guglielmone 1996; Sonntag et al. 2015; Fader et al. 2016). In the cortex, the PNNs are mostly in the primary sensory and motor areas, but fewer PNNs are present also in association areas (Brückner et al. 1999; Alpár et al. 2006).

PNNs are commonly associated with gamma-aminobutyric acid (GABA) containing neurons in the cortex (Yamada and Jinno 2013; Wolfgang Härtig, Brauer, and Brückner 1992; Lüth, Fischer, and Celio 1992), hippocampus (Du et al. 1996; Kawaguchi et al. 1987), thalamus (Hendry et al. 1988), brainstem or midbrain (Foster, Mellott, and Schofield 2014; Hilbig et al. 2007). These GABAergic neurons could be also distinguished by parvalbumin (PV) immunoreactivity (Kosaka and Heizmann 1989; Celio 1986). The calcium binding protein PV is responsible for buffering excessive calcium ions and limits repetitive release of GABA (Vreugdenhil 2002). These neurons are usually further associated with Kv3.1b subunit of potassium channel, when neurons containing Kv3.1b subunit are supposed to be fast-firing neurons (Morris and Henderson 2000). The pyramidal cells are sometimes also coated with PNNs (Alpár et al. 2006; Takahashi-Iwanaga, Murakami, and Abe 1998; Wegner et al. 2003) and simultaneously positive for Kv3.1b or contacted by Kv3.1b positive buttons (W. Härtig et al. 1999; W. Härtig et al. 2001). Localization of Kv3.1b subunit in the brain is for example in the olfactory bulb, neocortex, hippocampus, basal nuclei, septum, brainstem, cerebellum, thalamus, TB, superior and inferior colliculi (Weiser et al. 1995). It is evident that expression of Kv3.1b subunit corresponds with the localization of the PNNs. There are some more types of neurons that are surrounded by the PNNs such as glycinergic neurons of the TB (W. Härtig et al. 2001). On the other hand, PNNs are supposed to be devoid of cholinergic neurons (Adams et al. 2001).

On the scale of the neuron, PNNs ensheath soma, proximal dendrites and initial segment of an axon around some neurons (Sayed et al. 2002; Brückner et al. 2006; Brückner et al. 1996; Brauer et al. 1984) (Fig. 5). Another form of compact matrix is perinodal matrix at nodes of Ranvier (Cicanic, Sykova, and Vargova 2012; Bekku et al. 2010; Oohashi et al. 2002) and

axonal coats that could be found around axon terminals and synaptic boutons as focal ECM aggregates. They similarly contact mainly inhibitory terminals and could be integrated into the PNNs (Brückner, Morawski, and Arendt 2008).

3.2.2 Development

In the mouse primary visual cortex PNNs are visible initially between the postnatal day (P) 14 and P28. Around P42 the density of PNNs reaches the plateau. The expression of PV has a similar trend (Ye and Miao 2013). In the rat spinal cord PNNs become visible around P7 and are fully developed by P21 (Galtrey et al. 2008). Some components for the PNNs formation are present in the diffuse ECM even before the occurrence of the PNNs. However, aggrecan, TN-R, Crtl1 and Has expression is upregulated in concurrence with the onset of the PNNs formation (Carulli, Rhodes, and Fawcett 2007).

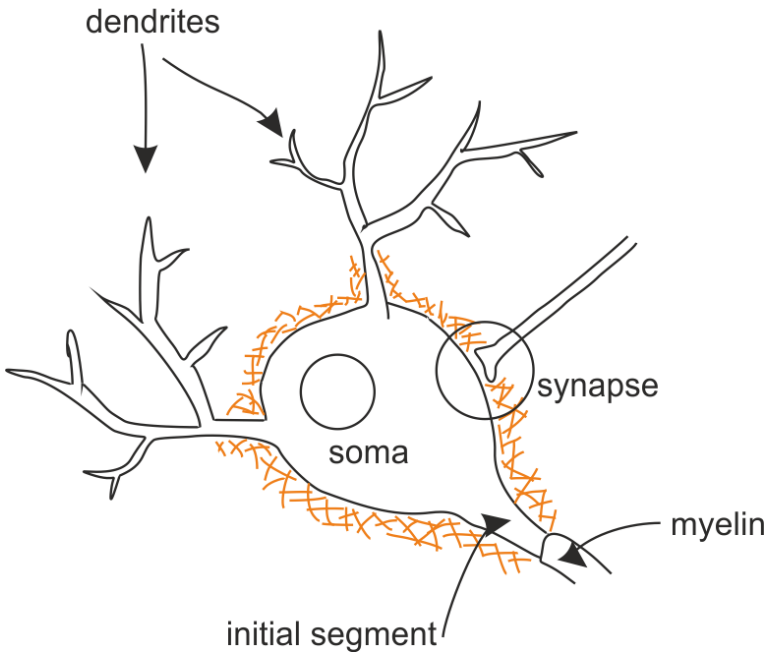

Figure 5: Localization of PNNs. PNNs (in orange) are localized around the soma of the neuron, proximal dendrites and initial segment. They are enwrapping the synapses. Source: author.

3.2.3 Physiological role

The function of the PNNs ensheathing neurons is very widespread and it seems that they play an important role in various processes during development, adulthood and ageing. The synaptic plasticity is very important feature of the neuronal net in the nervous system development, learning and memory formation or recovery from brain damage. In response to experience or damage, the neuronal net has an ability to change. During this process axon cones could grow and make new synapses and the existing synapses could undergo short-term or long-term synaptic potentiation or depression. During development there is a critical period when brain circuits are sensitive to experience and vast majority of synapses made in early postnatal life are subjects to synaptic pruning[1]. The brain neuronal circuits have an attempt to preserve active synapses. During particular time window the appropriate stimuli are necessary for correct maturation of the brain. In the CNS the formation of PNNs coincides with synaptogenesis in CNS (Blue and Parnavelas 1983) indicating that they may play a role in preserving of the synapses and in change of the diffusion conditions around these synapses. On the other hand, PNNs prevent axonal growth, thus they complicate regeneration within nervous system (Massey 2006). The formation of PNNs is with high probability regulated by the neurons themselves. When neurons are not active, the formation of PNNs is impaired. For example, dark rearing (from birth to P28) in mice lead to a reduced density of the PNNs (less aggrecan and TN-R staining) and decreased number of PV positive cells (Ye and Miao 2013). Another experiment comprising of the application of chondroitinase ABC (chABC) and monocular deprivation demonstrated that even in the adult visual cortex the ocular dominance could be induced after PNNs destruction (Pizzorusso et al. 2002). The results of Ye and colleagues (Ye and Miao 2013) could be explained by the study of Reimers et al. (Reimers et al. 2007), which states that chronic application of tetrodotoxin (TTX) (which is an inhibitor of voltage-gated sodium channels and therefore suppress neuronal activity) led to a later onset and slower formation of PNNs. Moreover, the chronic application of TTX resulted in a reduced *Wisteria floribunda* agglutinin (WFA) staining. Concomitantly, aggrecan as well as PV staining was impaired without a reduction of neuron density (Reimers et al. 2007). Another experiment used application of N-methyl-D-aspartate (NMDA) antagonist during P7 - P21 in

[1] Synaptic pruning is a process of competition among synapses (depending on neuronal activity) resulting in elimination of synapses.

hamster resulted in a reduced aggrecan staining around motor neurons. This was not observed in the adult animal (Kalb and Hockfield 1990) supporting the belief that PNNs formation depends on the conditions during critical period, but not afterward when PNNs are completely formed. On the other hand, the PNNs formation deficit *in vitro* and reduced frequency of IPSCs and EPSCs was observed in quadruple knockouts (deficient for brevican, neurocan, TN-R and TN-C). It is therefore evident that the PNNs are important for neuronal activity and synaptic strength (Geissler et al. 2013). One of the possible effects of PNNs on neuronal activity is their ability to influence the mobility of α-amino-3-hydroxy-5-methyl-4-isoxazolepropionic acid (AMPA) receptors. Enzymatic removal of the ECM with hyaluronidase increased exchange of extrasynaptic and synaptic AMPA receptors (in area per time unit) (Frischknecht et al. 2009).

Enzymes digesting the ECM help us to study its role within the CNS. Metalloproteinases (MMPs) (Nagy, Bozdagi, and Huntley 2007) - plasmin, disintegrins and metalloproteases (ADAMs) or ADAMs with trombospondin motif (ADAMTS) digest the ECM *in vivo* helping mainly in remodeling of synaptic circuits. Commonly used enzyme digesting PNNs is chABC, which disrupts the bonds between N-acetylgalactosamine and D-glucuronic acid, shortening the chondroitin sulfate chain (Köppe et al. 1997). Its effect lasts at least 7 weeks (Galtrey and Fawcett 2007) and then the PNNs are restored. The experiments with disruption of the PNNs during adulthood with chABC showed promising possibility to use matrix digesting enzymes in treatment of the brain injury as the destruction of PNNs with chABC after cervical spinal cord injury enhanced sprouting of axons (García-Alías et al. 2009). Likewise, application of chABC improved regeneration of nigral axons after axotomy in the CNS (Moon et al. 2001). These studies showed that degradation of CSPGs reduces their growth inhibiting properties and allows relearning without erasing the previous learned.

Very important function of PNNs is connected with negative charges carried by chondroitin sulfates (Brückner et al. 1993). Ionic bonding of positively charged ions to PNNs is important for regulation of diffusion of positively charged ions. For example, in the Bral1-deficient mice with a disruption of perinodal matrix, less effective conduction velocity was observed (Bekku et al. 2010). The existence of the PNNs is crucial for fast-spiking neurons with a low input resistance and high membrane potential that allows the leak of currents across the membrane (Kawaguchi and Kubota 1998; Balmer et al. 2009). The PNNs could trap molecules or even proteins in the vicinity of neuron. For example, Semaphorin3A (repulsive

axon guidance molecule) is seen around PV positive neurons co-localizing with the PNNs (Vo et al. 2013). Similarly, phosphacan binds with a high affinity a fibroblast growth factor-2 (Milev et al. 1998). PNNs are also important in binding of Oxt2 homeodomain protein, likely involved in PV positive cells maturation during the onset of the critical period (Beurdeley et al. 2012). Due to a large number of biding sites with a negative charge, the PNNs are able to bind cations, especially those with a higher valence. It was demonstrated that disruption of the PNNs with chABC led to an increased apparent diffusion coefficient for calcium ion and this change in local diffusion properties of calcium ion could affect synaptic transmission and neuronal excitability (Hrabetová et al. 2009).

As the PNNs stabilizes the synapses, they can contribute to the fixation of memory trails. Indeed, the impairment of LTP is seen in many ECM knockouts (Brakebusch et al. 2002; Zhou et al. 2001) and disruption of the PNNs in basolateral amygdala with chABC impairs fear memories, which are generally resistant to erasure in adult animals, suggesting promising opportunity for treatment of neurological disorders such as post-traumatic stress disorder (Gogolla et al. 2009). On the other side, PNN remodeling by MMPs is an important mechanism enabling an increase of the synaptic plasticity in response to a new stimulus. The role of MMPs was elucidated by Nagy and colleagues (Nagy, Bozdagi, and Huntley 2007) as they showed elevated expression and activation of MMPs after inhibitory avoidance training. Hippocampal stimulation by LTP-inducing stimuli led to increased expression/activation of MMP-9, potentially released by a postsynaptic neuron. This increase was necessary for LTP maintenance, but not for its induction (Bozdagi et al. 2007).

Last but not least, PNNs are seen as a protection against neurofibrillary degeneration. They are supposed to have antioxidant, anti-inflammatory and neuroprotective effects (Cabungcal et al. 2013). PNNs ensheathed neurons are less susceptible to accumulation of lipofuscin or to neuronal death caused by $FeCl_3$ injection, indicating the role of the PNNs in lowering of the effects of an oxidative stress (Morawski et al. 2004; Suttkus et al. 2012).

3.2.4 Diseases and PNNs

The most studied diseases connected to the PNNs are Alzheimer's disease (AD), schizophrenia and epilepsy. Postmortem studies of human brains revealed that people suffering

from schizophrenia have decreased PNNs densities by 70-76 % in layers 3 and 5 of the prefrontal cortex. However, the densities in visual cortex were unaffected (Mauney et al. 2013).

The digestion of the PNNs could be an useful tool to enhance plasticity (learning and memory) (Yang et al. 2015) in AD patients. However, the PNNs are also important for protection of the neurons and the treatment would be temporary. There is strong evidence that areas positive for the PNNs and CSPGs are less affected in the AD. They are devoid of hyperfosforylated protein Tau (Brückner et al. 1999) and they are less affected with lipofuscin (intralysosomal pigment) even in AD patients (Morawski et al. 2004). The essence of the AD pathology was linked to changes in the ECM molecules expression and PNNs, when Li and colleagues described altered distribution of Has1, which is most affected in the AD mice. Reduced number of Has1 on neuronal axons resulted in a shift from production of higher molecular weight HA to production of low molecular weight HA by Has3 in P301S Tau transgenic mice, showing that localization of Has is dependent on microtubules that are affected in the AD (Y. Li et al. 2017).

The development of epileptic seizures could be associated with altered GABAergic (inhibitory) signaling caused by decreased number of PNNs in medial prefrontal cortex of epileptic patients (Rankin-Gee et al. 2015). Application of AMPA receptor inhibitor, that is used to treat epilepsy, restored the density of PNNs (W. Chen et al. 2016).

The regulation of metalloproteinases expression could be changed in many neurological diseases. For example, there is a higher level of MMPs in the CNS of the patients with multiple sclerosis, malignant glioma or during ischemia, as well as a downregulation of inhibitors of these enzymes (Yong et al. 2001). We can therefore speculate that higher enzymatic degradation of protective PNNs during progression of these diseases could contribute to formation of "vicious circle" and aggravate the neuronal damage.

4. Central auditory system

Although a number of studies have shown the presence of the PNNs in hippocampus or visual cortex, nuclei of auditory system usually have more dense PNN expression (Sonntag et al. 2015). In our study we measured diffusion parameters in the IC and TB (Fig. 6). We chose IC as negative control as it is devoid of the PNNs containing Bral2 LP. The TB, on the other hand, has high expression of Bral2 LP and both nuclei posses Crtl1-aggrecan based PNNs.

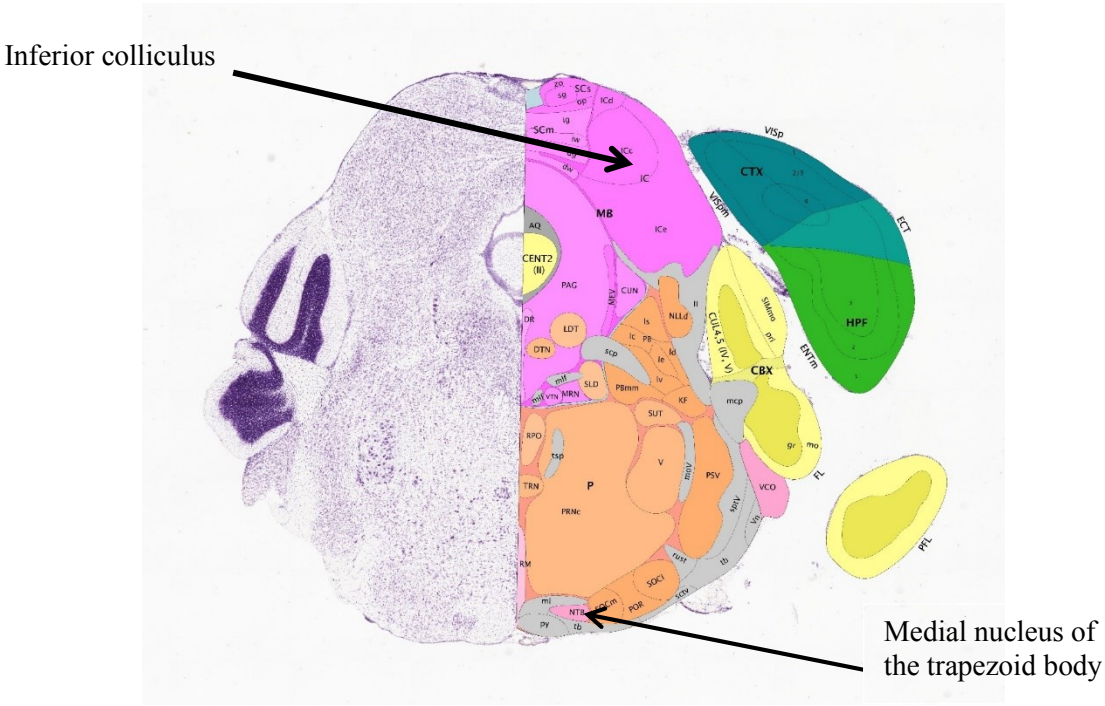

Figure 6: Coronal section across the brainstem. The two nuclei of interest are displayed with the arrows. Imported from Allen mouse brain atlas (Allen Institute for Brain Science 2011).

Many neurons in IC are GABAergic, positive for Kv3.1b subunit and surrounded with the PNNs (Foster, Mellott, and Schofield 2014; Hilbig et al. 2007). The IC has input from other brainstem nuclei and also from auditory cortex. The amount of inputs points out the role of IC in integration of information from auditory system and multi-modal integration.

Neurons of the TB are part of so called Calyx of Held, a big glutamatergic synapse between excitatory bushy cells from the contralateral cochlear nucleus and postsynaptic inhibitory glycinergic principal cells of the TB heading to the superior olivary complex. One presynaptic terminal contacts just one principal cell of the TB enwrapped in PNNs and expressing PV (Bekku et al. 2003; Blosa et al. 2013; Blosa et al. 2015). TB has a role in the sound localization. The presence of PNNs at calyx of Held may be associated with the velocity of synaptic transmission at calyx of Held, which is very fast, while brevican deficiency led to the reduced speed of the action potential transmission (Blosa et al. 2015). Due to the co-localization of brevican and Bral2 in the PNNs (Bekku et al. 2003), it is feasible to study

also the effect of Bral2 deletion and find out more about the changes that could lead to different effectivity of the synaptic transmission at the calyx of Held.

5. Aims of the thesis

The main goal of the project was to determine the role of Bral2 link protein in PNNs formation and stability, and to detect the effect of disruption of the PNNs on the ECS diffusion using the real-time iontophoretic method and immunohistochemical analysis.

The measurements were performed in two acoustic brainstem nuclei – medial nucleus of the trapezoid body and in inferior colliculus (set as a negative control). The further part of the project was focused on comparison of the effect of Bral2 deletion and enzymatical disruption with chondroitinase ABC on the ECS diffusion parameters and tissue structure.

Specific goals of my thesis were:

- To detect possible differences in the ECS diffusion parameters in the selected regions of interest between the young adult and aged wild type and Bral2-deficient mice
- To analyze the changes in the expression of the different ECM molecules in the Bral2-deficient tissue in comparison with the wild type one during adulthood and ageing
- To assess the aged-evoked changes of astrocytes in wild type and Bral2-deficient mice
- To compare the changes in diffusion parameters and expression of ECM molecules induced by Bral2 deficiency with those caused by enzymatic destruction of the PNNs by chondroitinase ABC

6. Methods

6.1 Animals

Bral2-deficient mice were generated by homologous recombination in embryonic stem cells, as described in (Bekku et al. 2012). The Bral2/Hapln4 gene was disrupted by inserting a promoterless IRES-tauLacZ gene and a floxed neomycin cassette into the Not I site of exon3, leading to the disruption of the immunoglobulin-like module. Control wild type mice of C57BL/6 strain and cryogenic preserved sperms of Bral2-deficient mice were kindly provided by our collaborating partner prof. Toshitaka Oohashi (Department of Molecular Biology and Biochemistry, Okayama University Graduate School of Medicine, Dentistry and Pharmaceutical Sciences; Okayama, Japan). To obtain *Bral2/Hapln4* deficient mice, we firstly generated heterozygous mice using *in vitro* fertilization of wild type mice with cryopreserved Bral2-deficient sperms. Heterozygous mice were then cross-bred and homozygous $Bral2^{-/-}$ and $Bral2^{+/+}$ (controls) animals were identified by genotyping (Fig. 7) and bred further. Two groups of different ages were measured and analyzed: 2-4 months old mice (young adult) and 12-18 months old mice (aged).

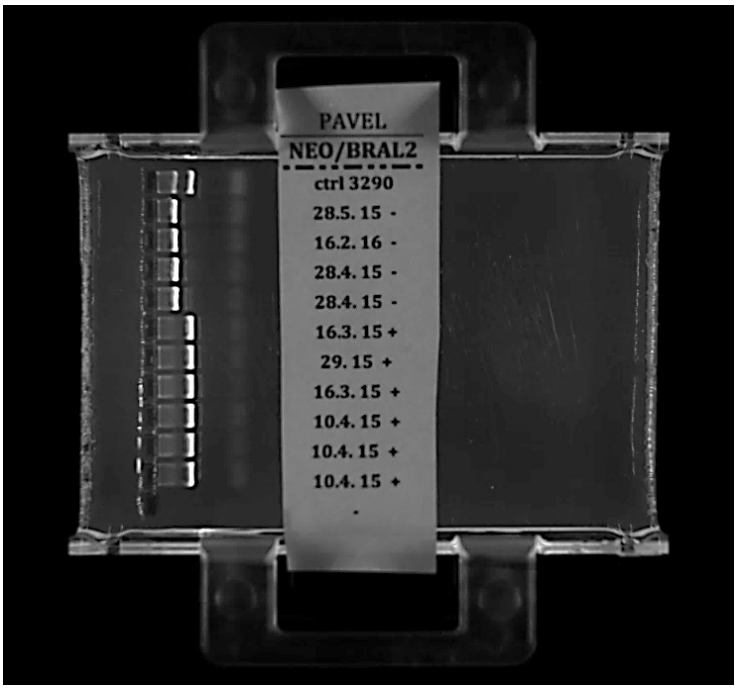

Figure 7: Results of polymerase chain reaction on gel after electrophoresis.

Genotyping of mice of different birth dates written on the paper in the middle (next to birth date is assumed presence or absence of *Hapln4* allele). Control band is present in the first row, followed by four assumed knockout mice lacking *Hapln4* allele and 6 mice with visible band corresponding with the control one.

6.2 Ion-selective microelectrodes

For our experiments, we use self-prepared ion-selective microelectrodes (ISMs) that are basically potentiometric sensors with membrane ideally selective for one specific ion. When the tip of ISM, that contains ion-selective exchanger and is backfilled with solution with known concentration of ion, is dipped into the solution with different concentration of measured ion, net diffusion of the permeant ion takes place through the membrane. This flux gives rise to a net movement of electrical charge and electric potential difference is generated across the membrane. Aligning the potential difference on both sides of the ion exchanger stops the net diffusion. The Nernst equation describes the size of this potential:

$$E = E_0 + s \log(a_i) \qquad (1) \quad ,$$

where E_o is the reference potential in millivolts, *s* is slope ($2.303\frac{RT}{zF}$) and a_i is the activity of the reference ion.

The Nernst equation has to be modified for exchangers because they are not fully ion specific and activities of all interacfering ions influence the final potential. The modified equation is called Nicolsky (Nicolsky-Eisemann) equation:

$$E = E_0 + s\log\left(a_i + \sum_i K_{ij}^{Pot}\left(a_j\right)^{z_i/z_j}\right) \qquad (2) \quad ,$$

where E is a potential measured on the amplifier side of the exchanger and E_0 is a constant potential difference that includes various interfacial potentials between the glass wall and electrolyte. The slope $s = 2.303\left(RT/z_iF\right)$, where R is the universal gas constant, T absolute temperature, z_i is the charge number of ion, F is a Faraday constant, a_j is the activity of *j*th interfering ion and K^{Pot}_{ij} is the potentiometric selectivity coefficient (influence of interfering ion). For simplification, activity is replaced with concentration of ion and the equation for two interfering ions could by written:

$$E_1 - E_2 = s\log(C_1 + k)/(C_2 + k) \qquad (3) \quad ,$$

where E_1 and E_2 are the potentials measured at the different concentrations (C_1, C_2) of the measured ion and k is interference (inserting the ISM into solution of different concentration is used for the electrode calibration).

As the electrode senses also biopotentials from the whole surrounding environment, the second, reference barrel, of the ISM measures these stable biopotentials (independent of composition and concentration of the sample), which are later subtracted from the ion-selective signal (Ch. Nicholson 1993).

Lux and Neher invented the basic principle of the method in 1973 using a K^+-ISM. In 1981, Nicholson and Phillips defined the real-time iontophoretic method using TMA^+-ISM

(Neher and Lux 1973; C. Nicholson and Phillips 1981), in which the K^+ ion exchanger (Corning 477317; Rochester, NY) was employed.

6.3 Measurement of ECS diffusion parameters

When diffusing, a substance is following a random path from regions with the higher concentration of the substance to the regions of its lower concentration. The Fick's laws describe diffusion in the free medium such as water (or diluted agar). However, the diffusion through the brain is hindered by many obstacles slowing down the velocity of diffusion and prolonging the path taken by the substance.

Basics of diffusion equations are obtained from Nicholson and Phillips (C. Nicholson and Phillips 1981).

Diffusion equations are based on the equation of the Fick's first law, which defines the microscopic Brownian motion of ions on macroscopic level.

Flux ($\overrightarrow{J}$) is defined as:

$$\overrightarrow{J} = -\mathrm{D}\,\nabla C_0 \qquad (4)\ ,$$

where D is diffusion coefficient for solute in water and C_0 is extracellular concentration and here is used ∇C_0 as a concentration gradient.

Extracellular space is very complex and the diffusing substance behaves differently than in free medium. Diffusion in brain may be described, when the diffusion parameters are introduced into diffusion equations. Extracellular volume fraction α is defined as:

$$\alpha = \frac{V_0}{V} \qquad (5)\ ,$$

where V represents volume of the tissue and V_0 is volume of the ECS. In aqueous solution or dilute gel α is supposed to be equal to 1.

The parameter of tortuosity expresses the ability of the ECS to prolong the diffusion path of substances. The tortuosity is defined as:

$$\lambda^2 = \frac{D}{D^*} \quad (6) \quad ,$$

where D is a diffusion coefficient in measured in free medium ($cm^2.s^{-1}$) and D* is an effective diffusion coefficient measured in the brain. The parameter D is higher than parameter D* because of the delay in the ECS.

From equation (1), the equation for isotropic porous medium could be modified by introduction of ECS diffusion parameters, as:

$$\overrightarrow{J} = -\alpha\, D^*\, \nabla C \quad (7) \quad ,$$

where α is a volume fraction, D* is an effective diffusion coefficient and C is the concentration of the substance in the ECS measured with the ISM.

From the second Fick's law we can estimate the simple diffusion equation to express α, λ and k':

$$\frac{\partial C}{\partial t} = D^* \nabla^2 C + \frac{Q}{\alpha} - k'C \quad (8) \quad ,$$

where Q is the volume average of source density in the medium. In that point the diffusion coefficient is reduced by the square of tortuosity, so that it is lower than in free medium. The source strength is reduced by the volume fraction, because the smaller the space into which we apply the substance, the higher the concentration in ECS seems to be. Parameter k' is uptake of the substance into the cell or across the blood-brain barrier.

The source can be defined as:

$$Q = {}^{In}/_{F} \quad (9) \quad ,$$

where I is the current, n is the transport number of the ISM and F is Faraday's electrochemical equivalent.

When current is applied TMA^+ ions are injected into the tissue during time course *S*. The change of the ion concentration (*C*) in the tissue is measured by the ISM at a distance (*r*). This change is displayed as a curve with rising and falling phase. For rising phase applies:

$$C = G(t) \qquad t < S \tag{10}$$

And for the falling phase of the curve it is:

$$C = G(t) - G(t - S) \qquad t > S \tag{11}$$

To obtain resolution of the diffusion curve function G (*u*), where $u = t$ (rising phase) or $u = t\text{-}S$ (falling phase) the modification of the first and second Fick's law was applied:

$$G(u) = (Q\lambda^2/8\pi D\alpha r) \tag{12}$$
$$\left\{\exp\left[r\lambda(k'/D)^{1/2}\right]\operatorname{erfc}\left[r\lambda/2(Du)^{1/2} + (k'u)^{1/2}\right] + \right.$$
$$\left.\exp\left[-r\lambda(k'/D)^{1/2}\right]\operatorname{erfc}\left[r\lambda/2(Du)^{1/2} - (k'u)^{1/2}\right]\right\}$$

where *Q* is the source strength (the amount of substance delivered per unit time into unit volume of tissue). There are parameters of tortuosity λ, volume fraction α, uptake k' and diffusion coefficient D. The function erfc is complementary error function.

6.4 Electrode preparation

The ion-selective electrodes were fabricated from borosilicate capillary glass (Ruckl and sons, Otvovice) 2.5 mm in diameter and 11 cm long. We made halves from the 11cm tube, put two tubes of different sizes together and fix them with polyethylene ring. The glass melts at relatively low temperatures so we can twist the pair around each other by 360°. We obtain two

double-barreled microelectrodes by pulling the twisted glass complex on vertical puller (Narishige, Japan).

Before the filling, the surface of glass has to be prepared for the ion exchanger. The glass surface is hydrophilic so that it would repel the organic liquid and have to be modified by the application of silane to the tip of the ISM making the ISM hydrophobic. We prepare the solution of reactive silicone tributylchlorosilane dissolved in organic solvent 1-chloronaphtalene (1:6, Fluka). Before silanization the reference barrel was filled with distilled water to obtain silanization of only one channel. The ISM was dipped into silane and one channel took in about 200-500 μm of the solution. The electrodes were heated in oven to 200°C for 1 hour to evaporate the liquid part and to let the silane create the hydrophobic surface in the tip.

After silanization electrodes were filled. First, we broke the tip against a glass tube under the microscope and back-filled the reference barrel with 150 mM NaCl solution. The ISM was then dipped into ion exchanger (IE 190, World Precision Instruments, RRID:SCR_008593) for few seconds and the ISM barrel was back-filled with 100 mM TMA^+-chloride solution. Potential air bubbles were removed by electrokauter or rat whisker.

Iontophoretic electrodes were made from theta-capillary double barrel borosilicate glass (EC1 30-0118, model TGC200-15, Harvard apparatus). The capillary was pulled on the vertical puller (Narishige, Japan) and bent to circa 40°. The tip was broken against a glass under the microscope and both barrels were back-filled with 100 mM TMA^+- chloride solution.

These two separate electrodes were glued together with parallel orientation of the tips, which were about 60-100 μm apart, using dental cement (Fig. 8).

The ISMs were calibrated in 5 solutions with different concentration of measured ion. From that calibration we obtained slope and interference of ISM by Nikolsky equation fitting using the software VOLTORO. The complete electrodes are calibrated in 0.1% agar (agarose with 1 mM TMA^+ in physiological saline containing 150 mM NaCl and 3 mM KCl) to acquire the exact distance of the tips (in μm) and transport number of the electrode from diffusion curves. Transport number of the electrode should be in the range 0.3-0.5. The occurrence of smaller transport number could mean a blockage of a channel while higher number indicates a significant bulk flow.

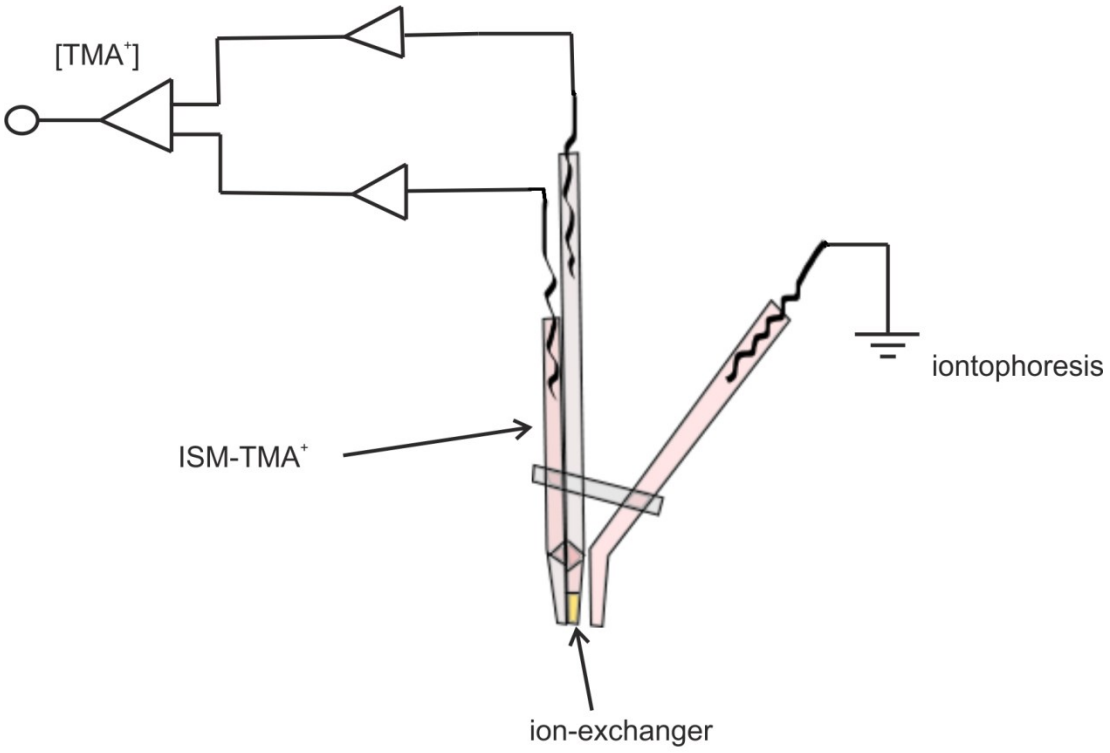

Figure 8: Scheme of the electrode. The electrode for real-time iontophoretic method consists of the ISM (on the left) and iotophoretic electrode (on the right). The ISM is made of two channels – reference and ion-selective. The reference channel is filled with 150 mM NaCl (grey color). The selective one contains ion exchanger at the tip (yellow color) and a solution of 100 mM TMA^+ chloride (pink color). Iontophoretic eletrode contains 100 mM TMA^+ chloride. The electrodes are connected to the differential amplifier with silver chlorinated wires. Source: author.

6.5 Detection of the ECS diffusion parameters

Both channels of the ISM were connected by silver chlorinated wires (Ag-AgCl) to the manufactured differential amplifier. Iontophoretic electrode was connected to a generator of rectangular electric current and the whole apparatus was grounded. We used a digital oscilloscope (model 310, Nicolet Instrument Corporation) to capture the curve and after transfer to the computer, the curve fitting was carried out in the VOLTORO program.

The TMA^+ ion was introduced to the tissue by an iontophoretic pulse and the concentration change in time at a known distance was detected with the TMA^+-ISM. Small bias current (20nA) was applied continuously in order to prevent changes in a transport number

when iontophoresis starts and to maintain the concentration of TMA^+ at the tip of the electrode constant. Iontophoresis duration was 24 seconds and the current was stepped to 200 nA.

From calibration in agar, where by definition $\alpha = \lambda = 1$ and $k' = 0$, we gained the values of the distance and transport number by a non-linear curve fitting. Knowing these parameters, we obtain values of α, λ and k' when the diffusion curve was recorded in the brain tissue. To measure the parameters with right diffusion coefficient we had to measure the temperature of the agar or the bathing solution. The examples of the diffusion curves recorded in the agar and brain tissue is shown in (Fig. 9).

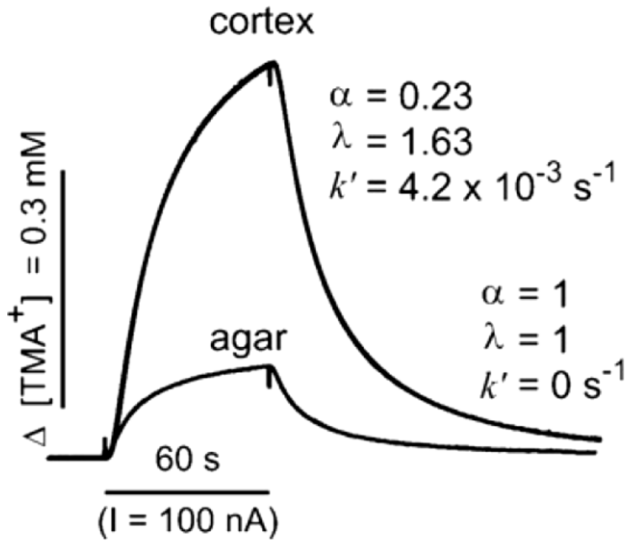

Figure 9: Diffusion curve for cortex and agar. Representative curve obtained in cortex and agar using iontophoretic method. The values showed here are mean values acquired in the cortex and diluted agar, representing medium with a free diffusion. Values of λ and α in the agar equal to 1, while that of uptake equals to zero. In the brain, α is smaller and λ higher due to the restriction of the diffusion only to the ECS and the presence of diffusion obstacles (cells, ECM). Taken from (Syková and Vargová 2008).

6.6 Acute brain slices

For acute brain slices of young mice, animals were anesthetized with ether, head was decapitated and the brain quickly isolated before cutting in a slicing solution. Old mice were deeply anesthetized by an intraperitoneal injection of pentobarbital (10 mg/ml) and perfused transcardially with 20 ml of N-methyl-D-glucamine (NMDG) solution before the decapitation.

During the isolation and cutting, brain was kept instantly in the ice-cold (4°C) slicing or NMDG solution. Coronal brain slices of 400 μm were cut on vibrating-blade microtome (Microm Int. GmbH, Waldorf, Germany). Subsequently, slices were incubated at least 1 hour in an artificial cerebrospinal fluid (aCSF) solution at room temperature. During measurements the slice chamber was instantly bathed by an aCSF containing 0.1 mM TMA^+ gassed with 95% O_2/5% CO_2. The measurements were carried out in a depth of 200 μm.

For the experiments with the enzyme chABC (Sigma Aldrich, C3667) the isolation and cutting of the brain was identical with the preparation of aged mice brain tissue. Slices were incubated in aCSF solution with 0.2 units/ml concentration of chABC for 2 hours at 37°C and later left for at least 60 minutes in aCSF at room temperature.

6.7 Solutions

NMDG solution composition: 110 mM NMDG, 2.5 mM KCl, 24.5 mM $NaHCO_3$, 1.25 mM Na_2HPO_4, 10 mM glucose, 7 mM $MgCl_2$, 0.5 mM $CaCl_2$ (pH = 7.4, 290 mOsm, bubbled by 95% O_2/5% CO_2).

Composition of aCSF solution: 154.5 mM Na^+, 3 mM KCl, 35 mM $NaHCO_3$, 1.3 mM Na_2HPO_4, 1.3 mM $MgCl_2$, 1.5 mM $CaCl_2$ (for slicing the $CaCl_2$ was not used, $MgCl_2$ was added instead of it), 10 mM glucose, 125.6 mM Cl^- (pH = 7.4, 290 mOsm, bubbled by 95% O_2/5% CO_2).

6.8 Tissue fixation and immunohistochemistry

Mice were anesthetized by intraperitoneal injection of the pentobarbital (10 mg/kg) and perfused transcardially with 20 ml of 0.9% physiological saline with heparin (2500 IU/100 ml) (Zentiva, Prague, Czech Republic) followed with the same amount of 4% paraformaldehyde solution in phosphate-buffered saline (PFA/PBS). The dissected brain was post-fixed in 4% PFA/PBS solution overnight. For cryoprotection, the tissue was placed in the PBS with gradually increasing sucrose concentration (10%, 20%) overnight. Twenty micrometers thick coronal slices were cut on cryostat microtome (MICROM cryostat). After the freezing medium was washed out, slices were incubated for 2 hours in blocking medium containing 5% Chemiblocker, 0.2% Triton and 10% goat or donkey serum (donkey serum is used for goat antibody anti-Crtl1) in PBS-glycine (in PBS for Crtl1 staining). After blocking, slices were

incubated overnight at 4°C with a primary antibody. The antibodies used were: goat anti-Bral2 (AF4085; 1:300; R&D systems); goat anti-Crtl1 (AF2608; 1:150; R&D systems); rabbit anti-brevican (Ab111719; 1:100; Abcam); rabbit anti-aggrecan (Ab1031; 1:1000; Millipore). After washing out, slices were incubated with a secondary antibody for 2 hours at 4°C in PBS containing 0.2% Triton. Secondary antibodies were: g488 for Bral2 (1:200), d488g for Crtl1 (1:300), g488R for brevican (1:200), g488R for aggrecan (1:200). To visualize the cell nuclei, 4', 6-diamidino-2-phenylindole (DAPI) was applied for 10 seconds on the slice and the slice was mounted on microscope slides with a mounting solution Aqua-Poly/Mount (Polysciences Inc.).

The procedure for GFAP staining was similar, however, as the antibody mGFAP Cy3 (1:400; Sigma-Aldrich) is conjugated with Cy3 dye, secondary antibody was not required.

WFA staining procedure was slightly different. Slices were preincubated in 0.1M PBS containing 1% H_2O_2 for 10 minutes. The blocking was carried out in the solution containing 0.3% Tritone and 3% goat serum for 1 hour. Incubation with biotinylated WFA (1:200; Sigma-Aldrich) was carried overnight at 4°C and as a secondary antibody was used Streptavidin 488 (SA-5488; 1:200; Vector).

6.9 Image analysis

To quantify the differences in ECM molecules expression between WT mice and Bral2-deficient mice, the slices were scanned using the fixed entrance conditions on EVOS® FL Auto microscope (Thermo Fisher Scientific). Measurement of the area comprising GFAP positive cells, counting of GFAP positive cells and analysis of mean intensity of staining were performed using an ImageJ software (ImageJ, RRID:SCR_003070). The images were segmented using Li's Minimum Cross Entropy thresholding method (C. H. Li and Tam 1998). Area of GFAP staining was analyzed using an intrinsic ImageJ area measurement tool, cell counting was performed manually assisted by a Cell Counter plugin. Morphometric analysis of GFAP labeled astrocyte processes was performed by measuring the diameter of the thickest process at a location 10-15 μm away from the nucleus (one half of the astrocyte domain radius).

6.10 Data analyses

Data were analyzed by unpaired t-test using GraphPad InStat software (GraphPad Software, USA). P values under 0.05 were considered statistically significant. P values under 0.01 were considered very statistically significant. P values under 0.0001 were considered extremely statistically significant. Data are presented as mean ± standard error of the mean. Graphs were created using MS Excel and CorelDraw.

7. Results

7.1 ECS volume fraction and tortuosity in Bral2-deficient mice and controls

RTI method was employed to determine the diffusion parameters in the IC and TB of the WT and Bral2-deficient mice (knockout, KO). The IC represents the negative control as it is devoid of Bral2 based PNNs. Firstly, we studied the effect of Bral2 deletion in young mice (3 months old), where we have not observed any change in the ECS diffusion parameters between the WT and KO mice either in the TB or IC (Table 1.; Fig. 10). As shown in a previous study of our lab, aging might be crucial in revealing of the hidden changes evoked by Bral2 deficiency (Cicanic et al., submitted). Therefore, the aged animals (12-18 months old) were included to the study. Aging evoked a typical decrease in the ECS volume fraction in both studied regions of interest in the KO but not in the WT mice. We discovered a significant decrease in tortuosity in the TB of the aged KO mice. We observed aging related increase in tortuosity in all studied groups. However, the age related tortuosity increase in the TB of the WT mice was more prominent than in their aged-matched controls (Table 1.; Fig. 11).

Table 1. TMA^+ diffusion parameters measured in mouse brain slices using the RTI method

Region	age		α	λ	*n*	No. of mice
Inferior colliculus	young	WT	0.170 ± 0.007	1.659 ± 0.025	22	11
	aged	WT	0.162 ± 0.007	1.743 ± 0.027	26	12
	young	KO	0.189 ± 0.007	1.655 ± 0.017	21	10
	aged	KO	0.157 ± 0.007	1.766 ± 0.025	28	16
Trapezoid body	young	WT	0.186 ± 0.015	1.680 ± 0.027	19	11
	aged	WT	0.158 ± 0.008	1.876 ± 0.033	21	10
	young	KO	0.227 ± 0.022	1.678 ± 0.028	8	7
	aged	KO	0.141 ± 0.012	1.789 ± 0.025	22	10

Data are expressed as mean ± SEM. The number of measurement from each insert was *n* and several were made in each slice.

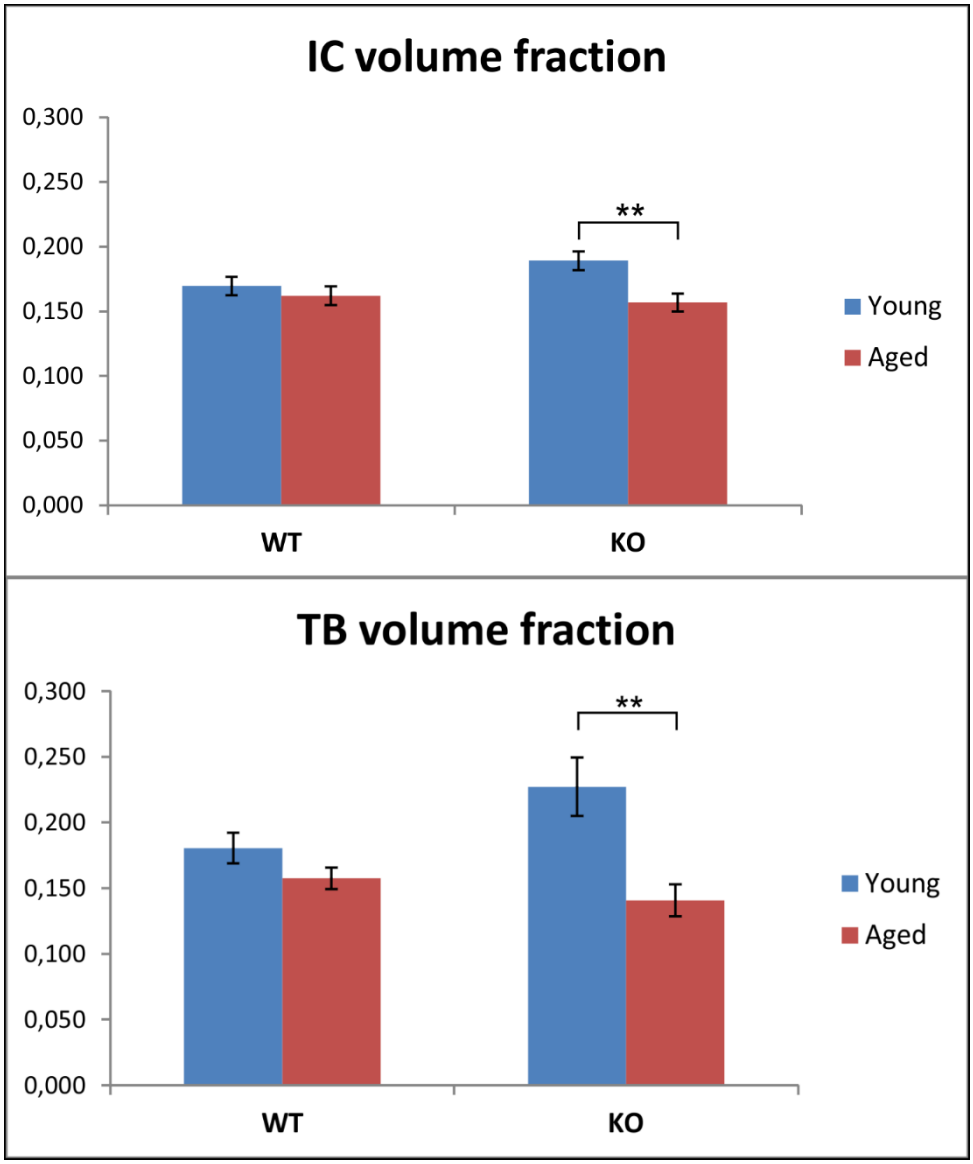

Figure 10: Comparison of the mean values of the ECS volume fraction. The mean values of the ECS volume fraction in the inferior colliculus (IC) and the trapezoid body (TB) of the wild type (WT) and Bral2-deficient mice (KO). Data are given as mean ± SEM. P values under 0.01 were considered very statistically significant (**, $P \leq 0.01$). SEM - standard error of the mean

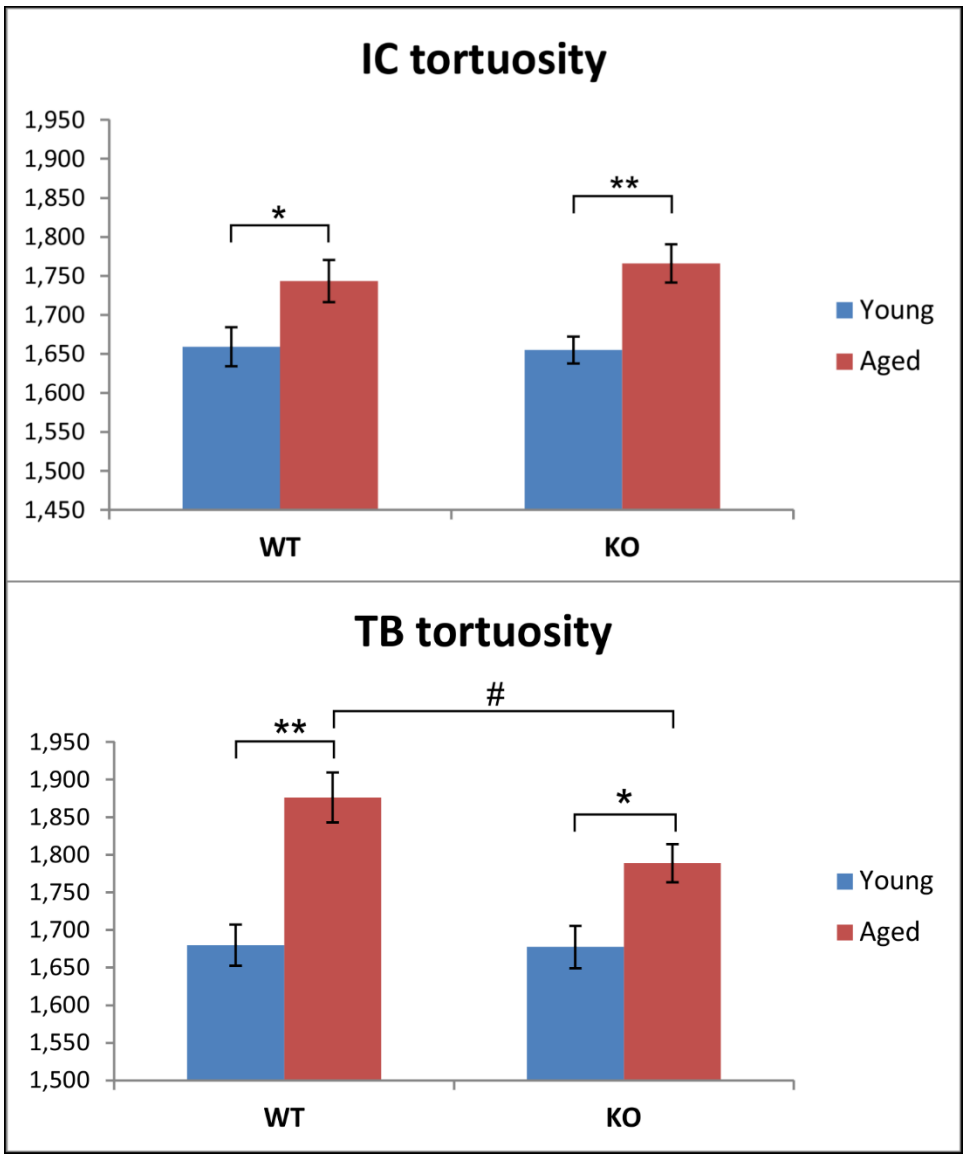

Figure 11: Comparison of the mean values of tortuosity. The mean values of tortuosity in the inferior colliculus (IC) and the trapezoid body (TB) of the wild type (WT) and Bral2-deficient mice (KO). * marks a significant difference between young and old mice, # marks a significance between WT and Bral2-deficient mice. Data are given as mean ± SEM. P values under 0.05 were considered statistically significant (*, #; $P \leq 0.05$). P values under 0.01 were considered very statistically significant (**, $P \leq 0.01$). SEM - standard error of the mean

7.2 ECM molecules expression in Bral2-deficient mice

To study the differences in the level of expression of the distinct ECM molecules between the WT and KO mice in the TB and IC of the young and aged animals, we employed the immunohistochemical analysis of the fluorescent microscope scanned images. As the missing link protein Bral2 in the ECM complexes might be replaced by Crtl1, we assessed the expression of these two LPs as well as of the lecticans, which often co-localize with them: brevican and aggrecan, respectively. The PNNs based on Crtl1 and aggrecan were discovered in both regions of interest (Figs. 14 and 15). Additionally, we observed the PNNs based on Bral2 and brevican in the TB. The IC was devoid of the Bral2-brevican based PNNs and served as a negative control (Figs. 12 and 13). In comparison with the WT animals, the Bral2-based PNNs diminished in the TB of the KO animals, however, Crtl1-aggrecan based PNNs were still present in the KO mice. Brevican expression in the KO mice loose its typical PNN-like pattern, but diffuse brevican positivity was detected in the ECS (Fig. 13).

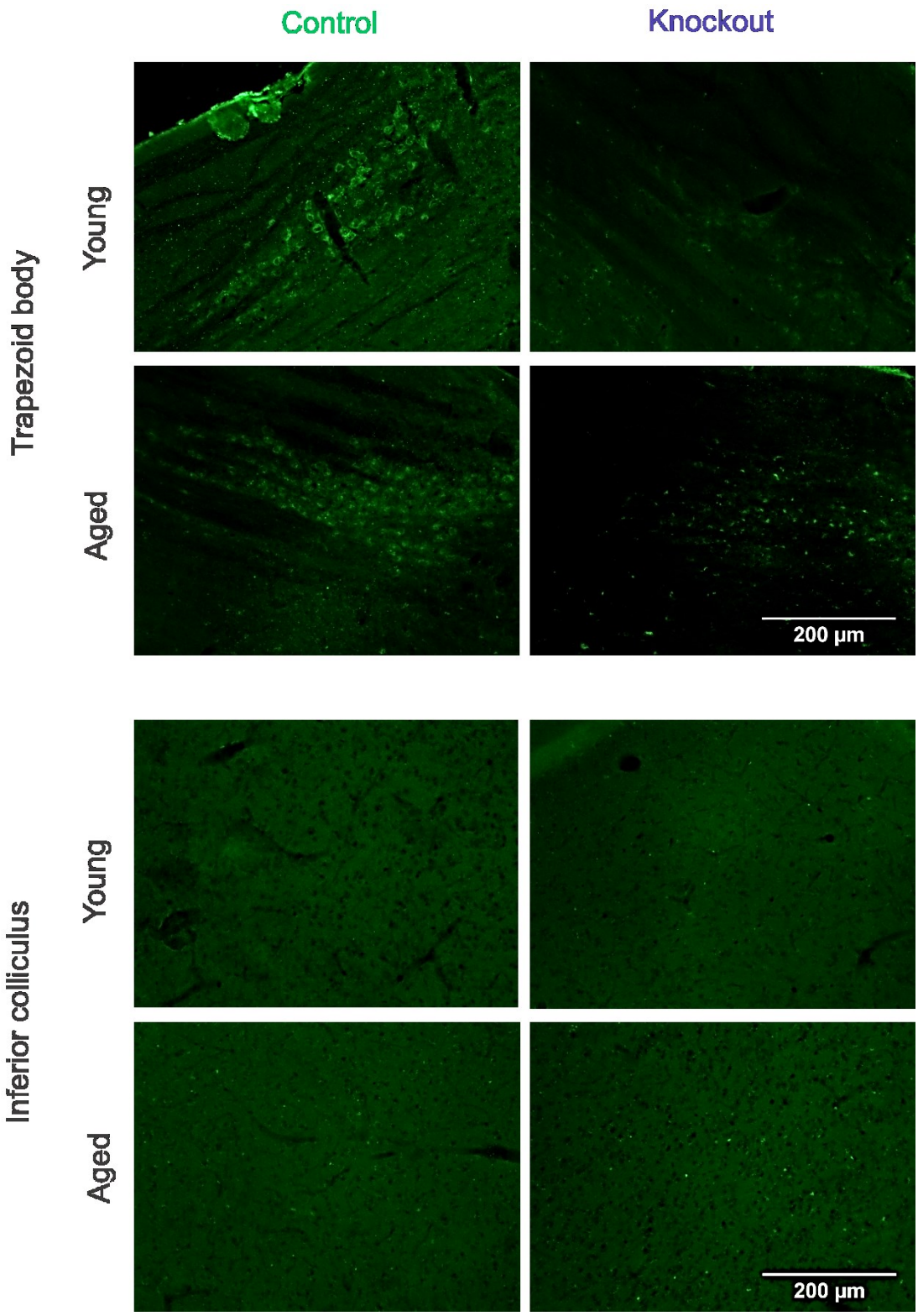

Figure 12: Comparison of Bral2 protein expression in the young and aged wild type and knockout mice in the TB and in the IC. The scale is depicted in the image. The images of the TB and IC were taken using the same objective magnification.

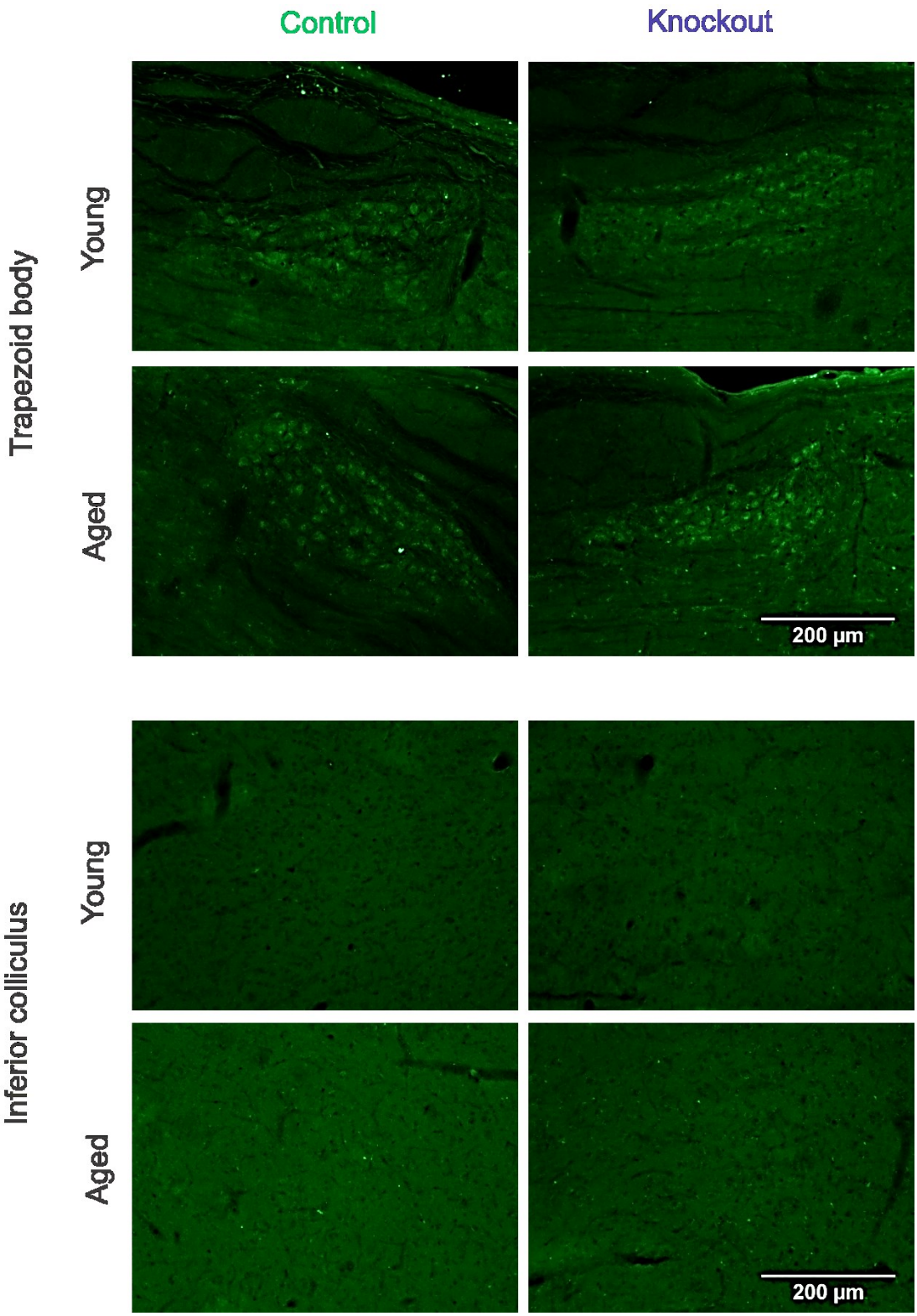

Figure 13: Comparison of brevican protein expression in young and aged control and knockout mice in the TB and in the IC. The scale is depicted in the image. The images of the TB and IC were taken using the same objective magnification.

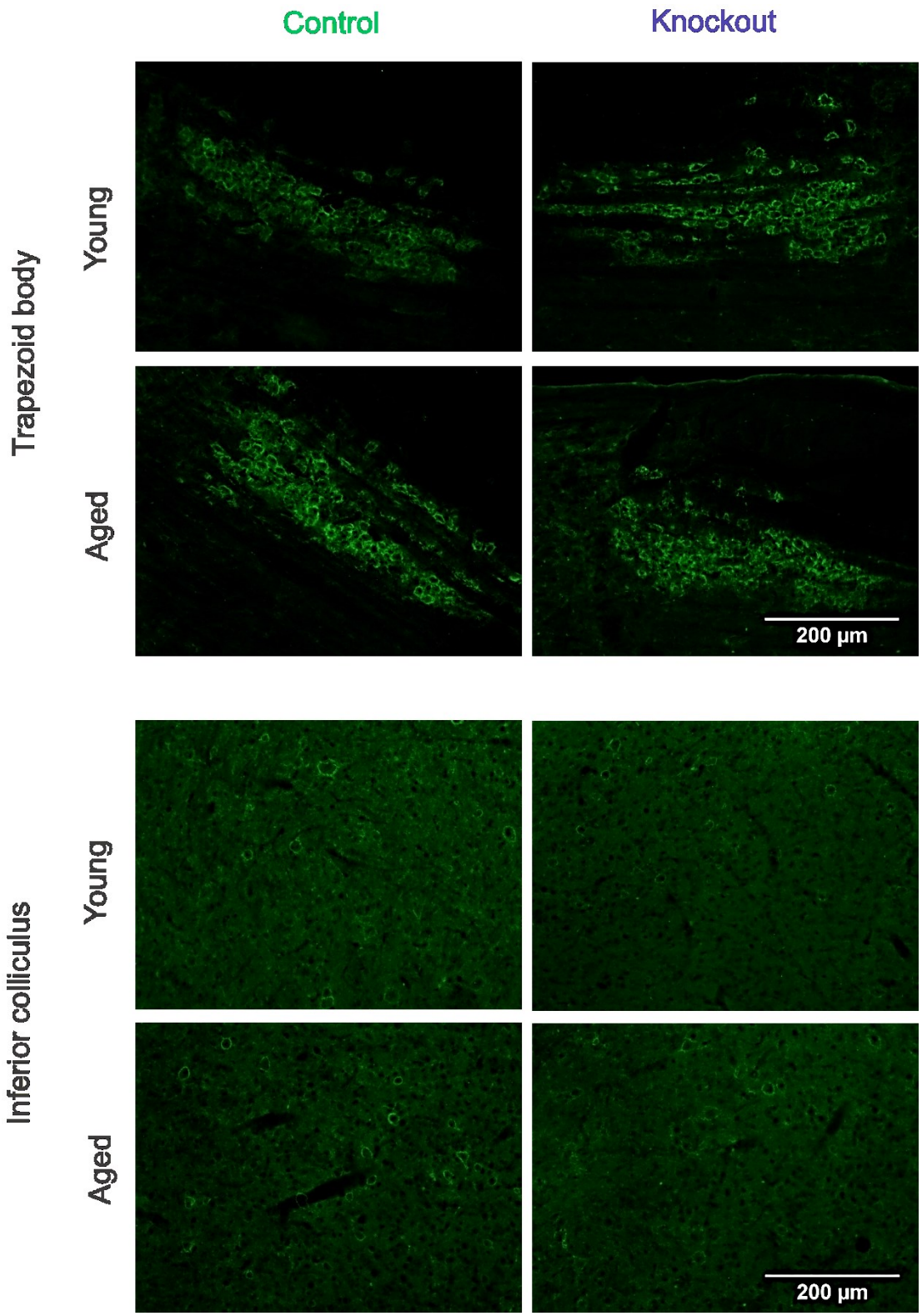

Figure 14: Comparison of Crtl1 protein expression in young and aged control and knockout mice in the TB and in the IC. The scale is depicted in the image. The images of the TB and IC were taken using the same objective magnification.

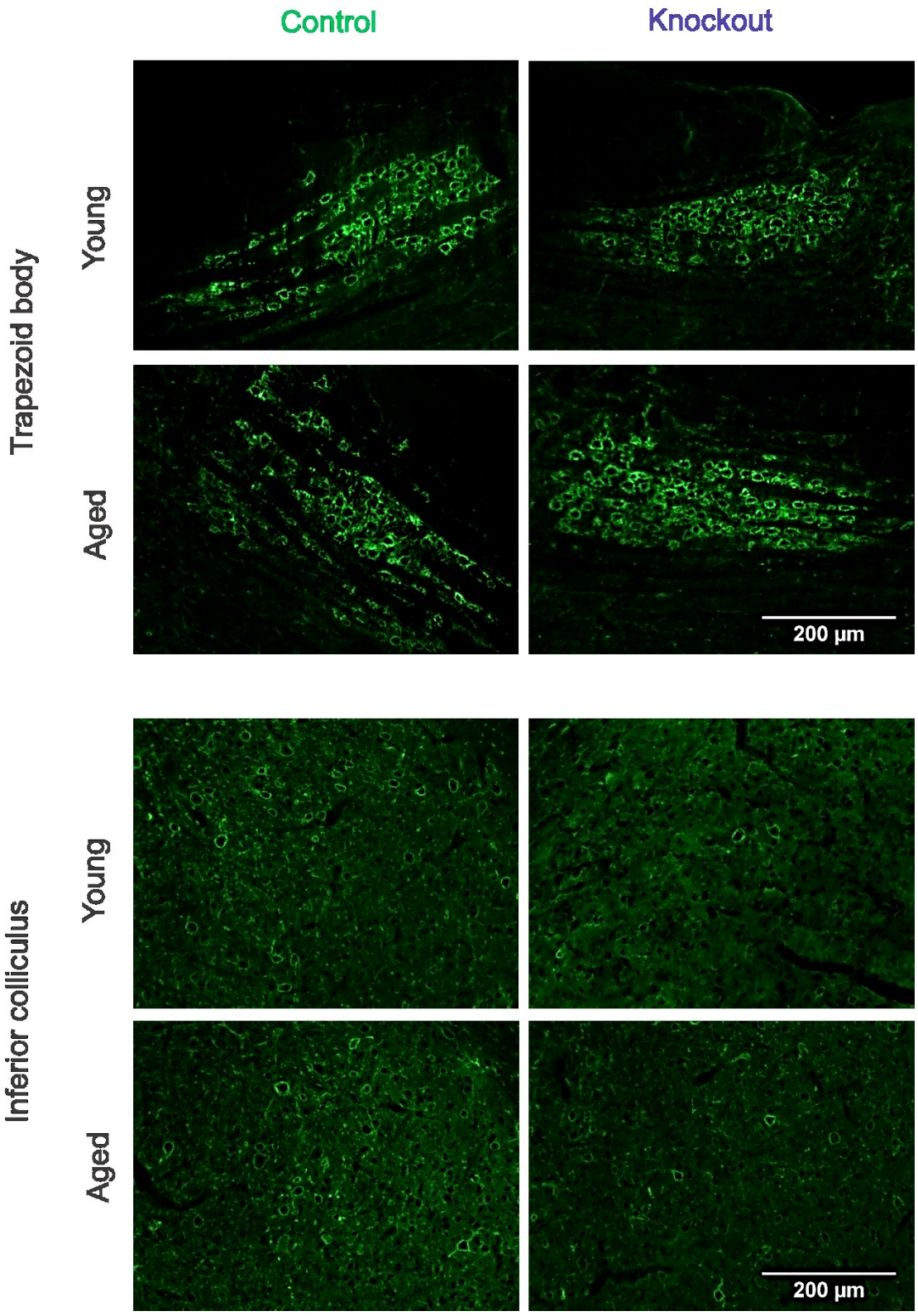

Figure 15: Comparison of aggrecan protein expression in young and aged control and knockout mice in the TB and in the IC. The scale is depicted in the image. The images of the TB and IC were taken using the same objective magnification.

To further analyze the changes in the expression of these four proteins, we quantified their staining. The mean staining intensity value obtained in the young WT TB mice was set as 1 and staining intensity values in all other groups were related to 1.

As the Bral2 based PNNs diminished in the KO animals and the IC is devoid of Bral2 based PNNs (see Fig. 13 above), we have analyzed the Bral2 expression only in the young and aged WT mice TB, where we discovered no significant change in its staining intensity (Fig. 16). The further analysis did not show any significant change of brevican, aggrecan or Crtl1 staining intensity (Figs. 17-19).

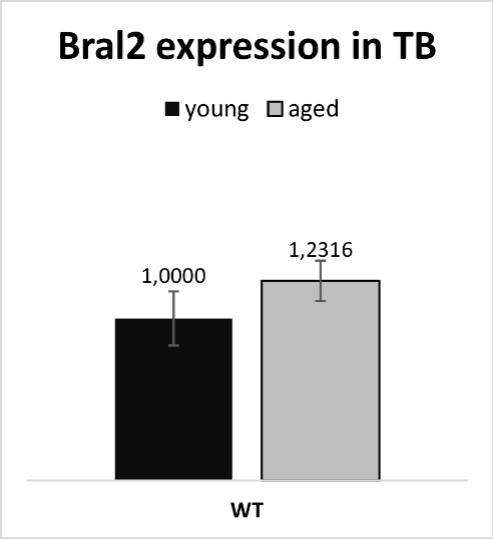

Figure 16: Bral2 protein expression in the young and aged WT mice in the TB. All values are related to 1 (young WT mice). WT - wild type; TB - trapezoid body.

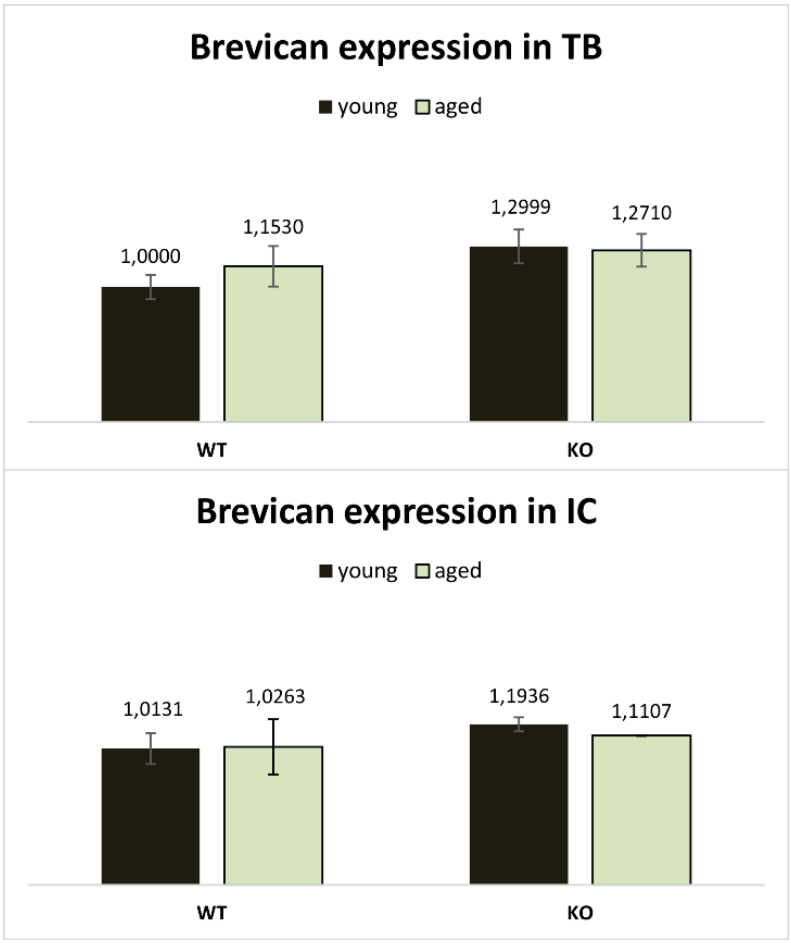

Figure 17: Brevican expression in the WT and KO mice. All values are related to 1 (young WT mice in the TB). WT - wild type; KO - knockout; IC - inferior colliculus; TB - trapezoid body.

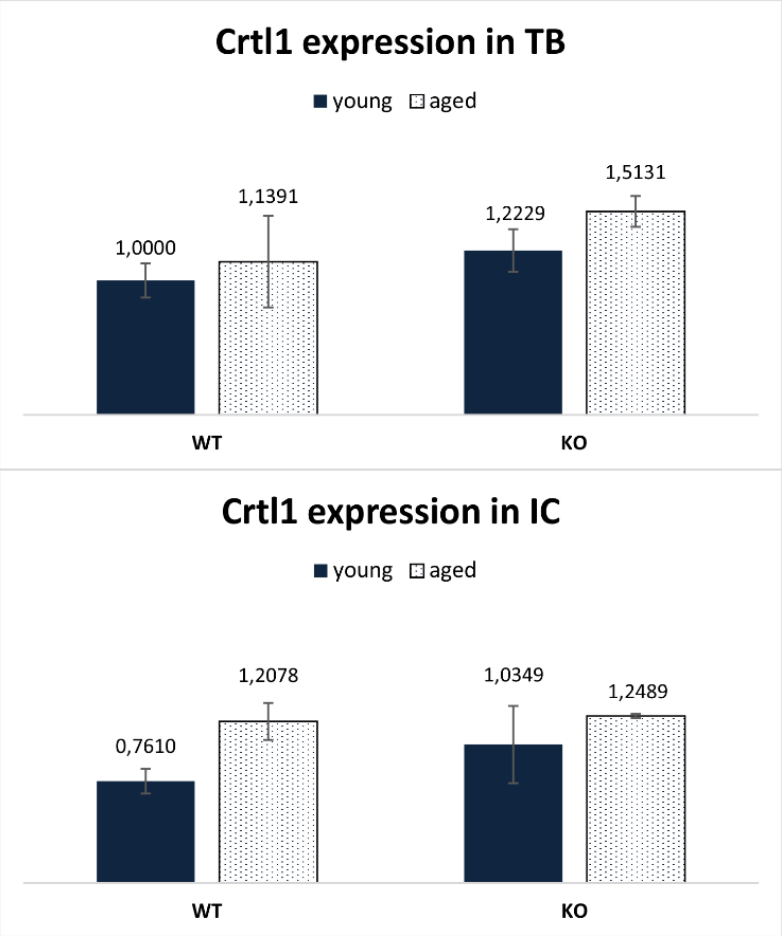

Figure 18: Crtl1 expression in the WT and KO mice. All values are related to 1 (young WT mice in the IC or the TB). WT - wild type; KO - knockout; IC - inferior colliculus; TB - trapezoid body.

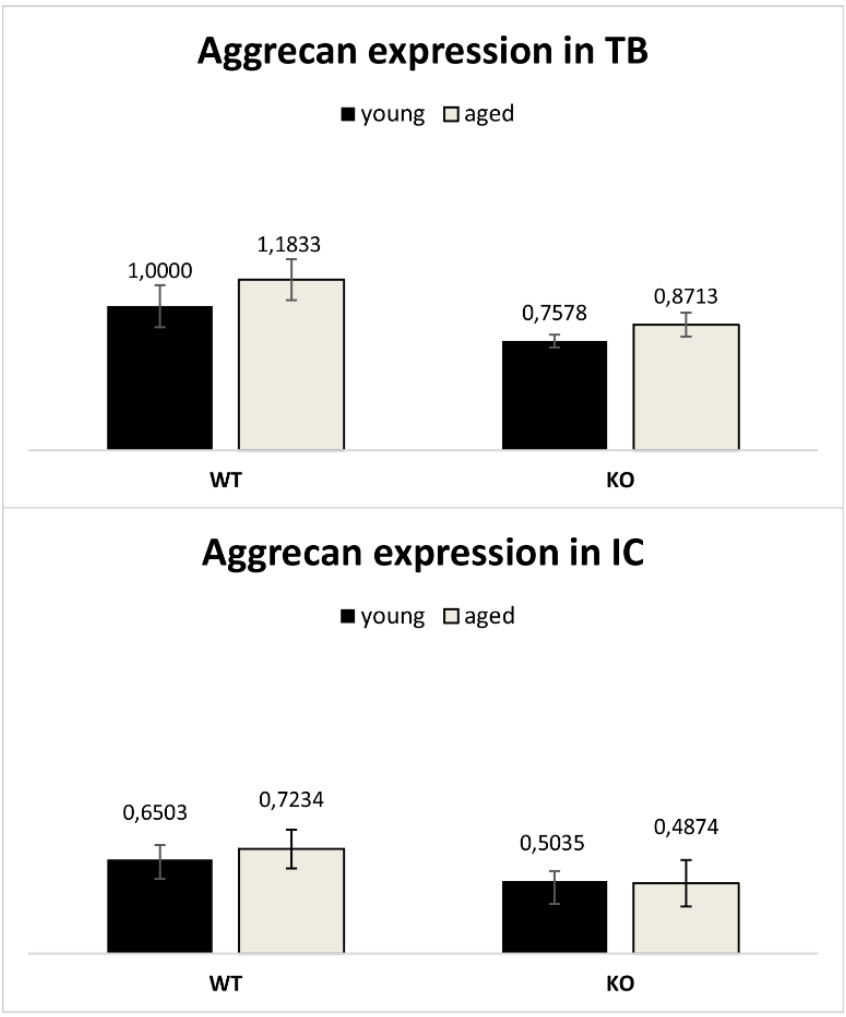

Figure 19: Aggrecan expression in the WT and KO mice. All values are related to 1 (young WT mice in the IC or the TB). WT - wild type; KO - knockout; IC - inferior colliculus; TB - trapezoid body.

7.3 GFAP positive cells in the Bral2-deficient mice

As ageing are often related to astrogliosis-like changes, the staining for GFAP was performed to assess differences in the astrocyte morphology between the WT and KO mice in the young and aged IC and the TB. In the young IC, we observed just few GFAP positive cell and their number seems to increase during aging. However, we performed the staining procedure on two available aged mice, which showed the great variability in the GFAP positive cell density. The TB was far richer on the GFAP positive cell than the IC and their number have not differ between the young and aged WT or KO animals (Figs. 20-21).

We did not show significant increase in GFAP positive cell number in the TB or IC during aging. In the IC, the width of the processes did not differ. However, in the TB, we observed a decrease of the width in the KO animals that was significant in the young KO mice. The width of the processes was increasing with age in the TB, with significant increase from young to aged KO animals (Figs. 22-23).

In the IC, we have shown significantly increased surface area in aged WT animals as compared with the age-matched controls. In case of the surface area of the GFAP positive cells in the TB, we observed significantly increased size in aged animals as compared to the young ones. However, the overall size was lower in the KO mice as compared to the age-matched controls with significantly decreased surface area in the aged KO as compared with the aged WT animals (Figs. 22-23).

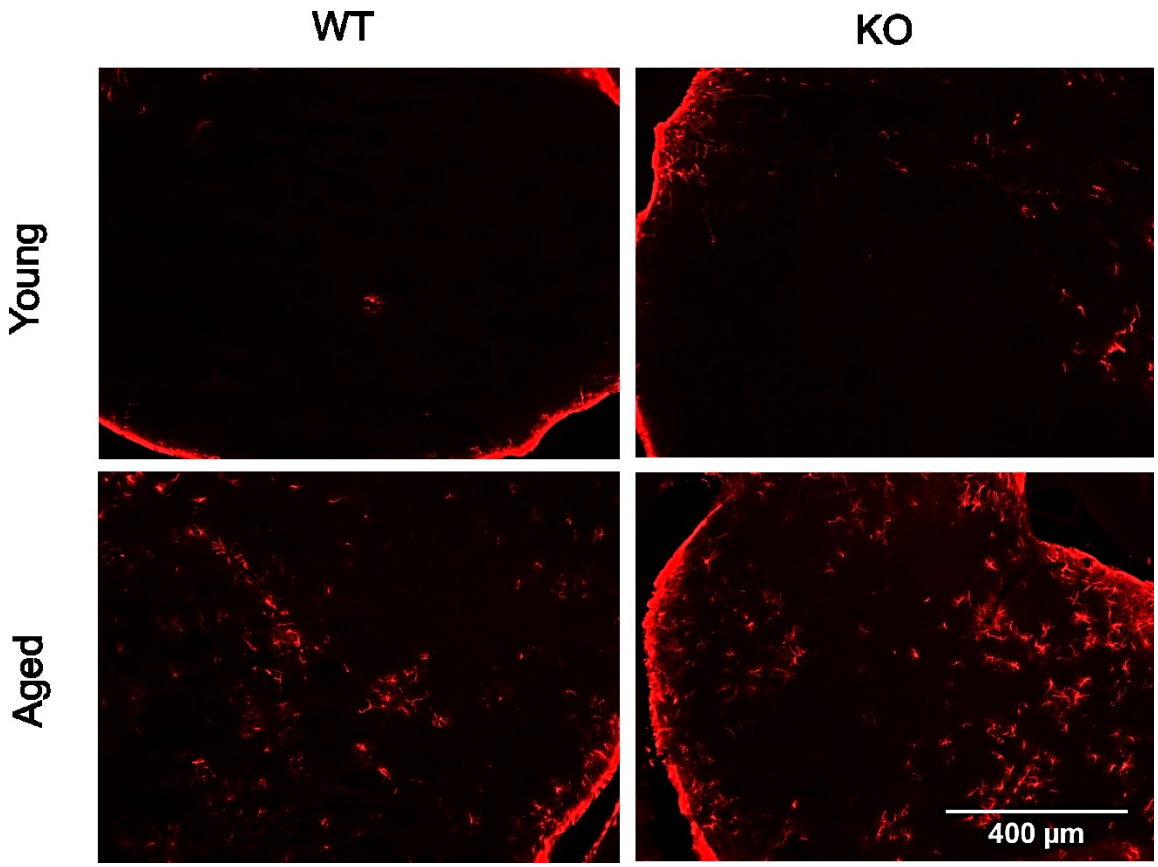

Figure 20: GFAP staining in the inferior colliculus. The scale is depicted in the image. WT - wild type; KO - knockout; IC - inferior colliculus

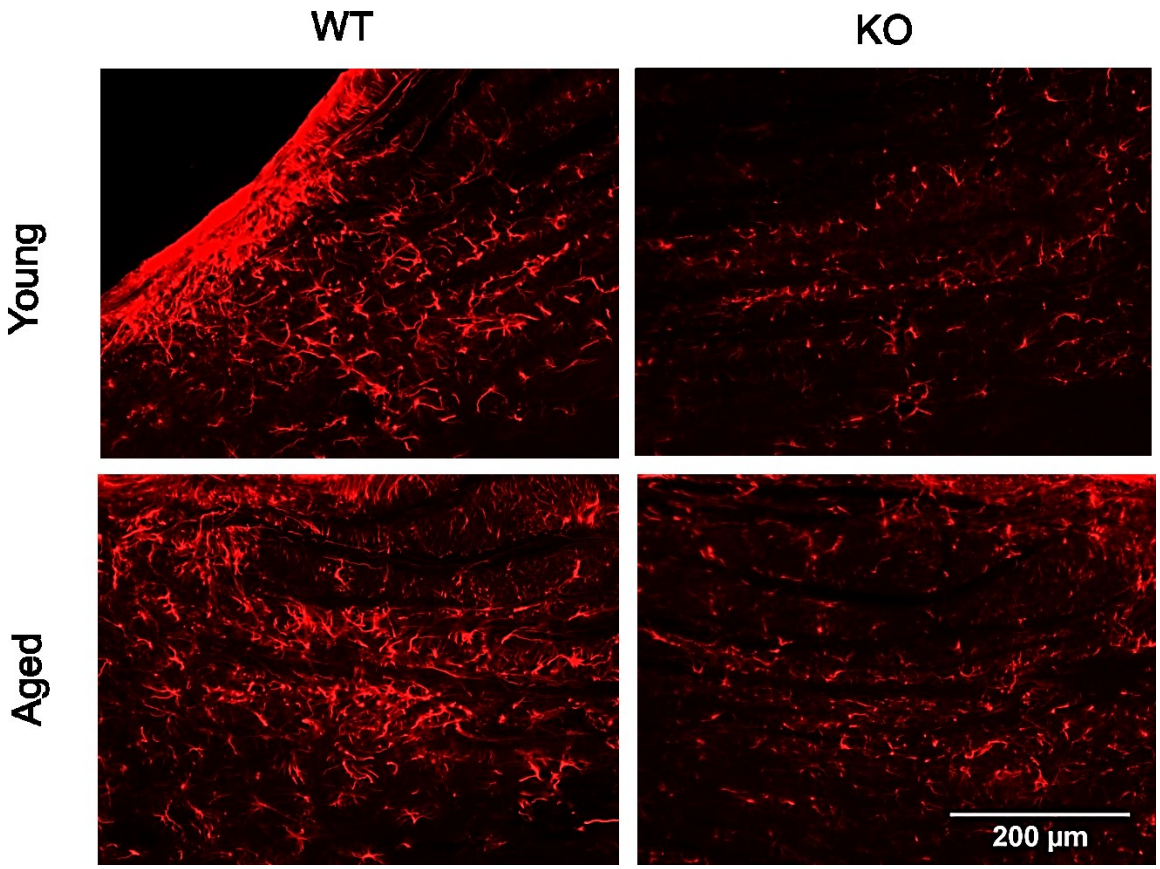

Figure 21: GFAP staining in the trapezoid body. The scale is depicted in the image. WT - wild type; KO - knockout; TB - trapezoid body.

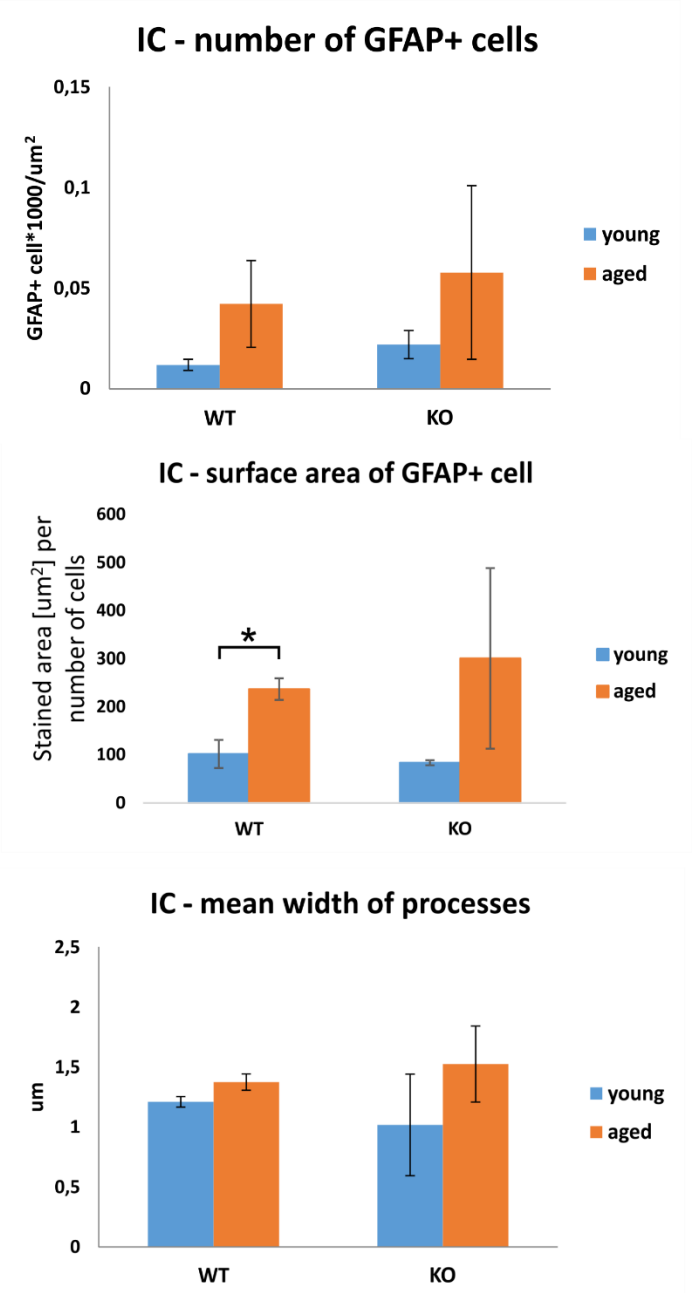

Figure 22: GFAP positive cells in the inferior colliculus. GFAP positive cell density, mean surface area of single GFAP positive cell and the mean width of the processes in the inferior colliculus (IC) of the wild type (WT) and Bral2-deficient mice (KO). Data are given as mean ± SEM. P values under 0.05 were considered statistically significant (*, $P \leq 0.05$). SEM - standard error of the mean

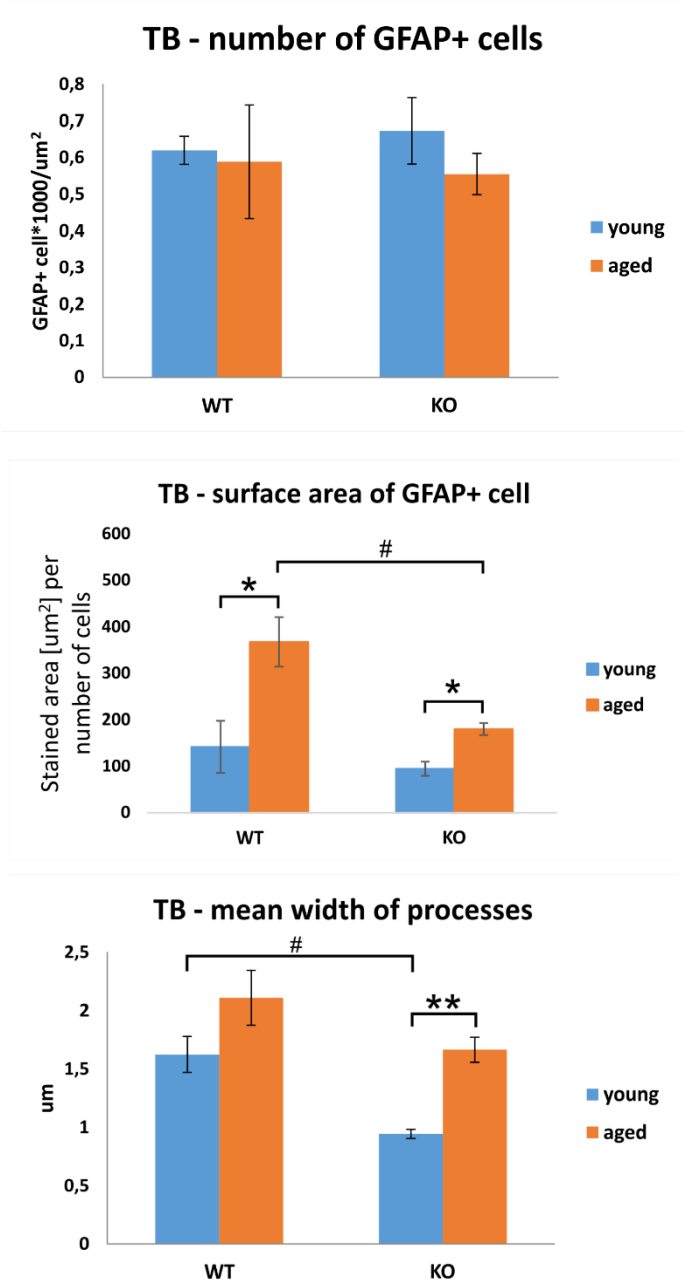

Figure 23: GFAP positive cells in the trapezoid body. GFAP positive cell density, mean surface area of single GFAP positive cell and the mean width of the processes in the trapezoid body (TB) of the wild type (WT) and Bral2-deficient mice (KO). Data are given as mean ± SEM. * marks a significant difference between young and old mice, # marks a significance between WT and Bral2-deficient mice. P values under 0.05 were considered statistically significant (* or #, $P \leq 0.05$). P values under 0.01 were considered statistically significant (**, $P \leq 0.01$).

7.4 Diffusion parameters in the chondroitinase ABC treated mice

To assess the effect of enzymatic disruption of the ECM complexes on the ECS diffusion, we measured the ECS volume fraction and tortuosity changes in the young (3-5 months old) and aged (12-18 months old) WT animals after the administration of enzyme chABC into the incubation bath. The measurements from WT mice of the matched age obtained above were used as a control.

The mean values of the ECS diffusion parameters before and after chABC treatment are shown in Table 2. Figures 25 and 26 depict the values of the ECS diffusion parameters from the WT and KO animals (chapter 7.1) as we have compared them to the ECS diffusion parameters measured in the slices that were incubated with chABC.

There was no difference in the ECS diffusion parameters between the young and aged animals treated with chABC. The values of tortuosity was significantly increased in the chABC treated animals as compared to the WT and also to the KO mice in all studied groups. In the young animals, we have detected a lower ECS volume fraction in the chABC treated animals in the comparison with the KO mice (Figs. 24 and 25).

Table 2. TMA^+ diffusion parameters measured in the inferior colliculus and trapezoid body in mouse brain slices using the RTI method

Region	age	chABC	α	λ	*n*	No. Of mice
Inferior colliculus	young	No	0.170 ± 0.007	1.659 ± 0.025	22	11
	aged	No	0.162 ± 0.007	1.743 ± 0.027	26	12
	young	Yes	0.152 ± 0.014	1.995 ± 0.074	12	5
	aged	Yes	0.159 ± 0.011	2.050 ± 0.071	9	4
Trapezoid body	young	No	0.181 ± 0.012	1.680 ± 0.027	19	11
	aged	No	0.158 ± 0.008	1.876 ± 0.033	21	10
	young	Yes	0.152 ± 0.020	2.166 ± 0.125	7	4
	aged	Yes	0.167 ± 0.014	2.203 ± 0.124	6	3

Data are expressed as mean ± SEM. The number of measurement from each insert was *n* and several were made in each slice.

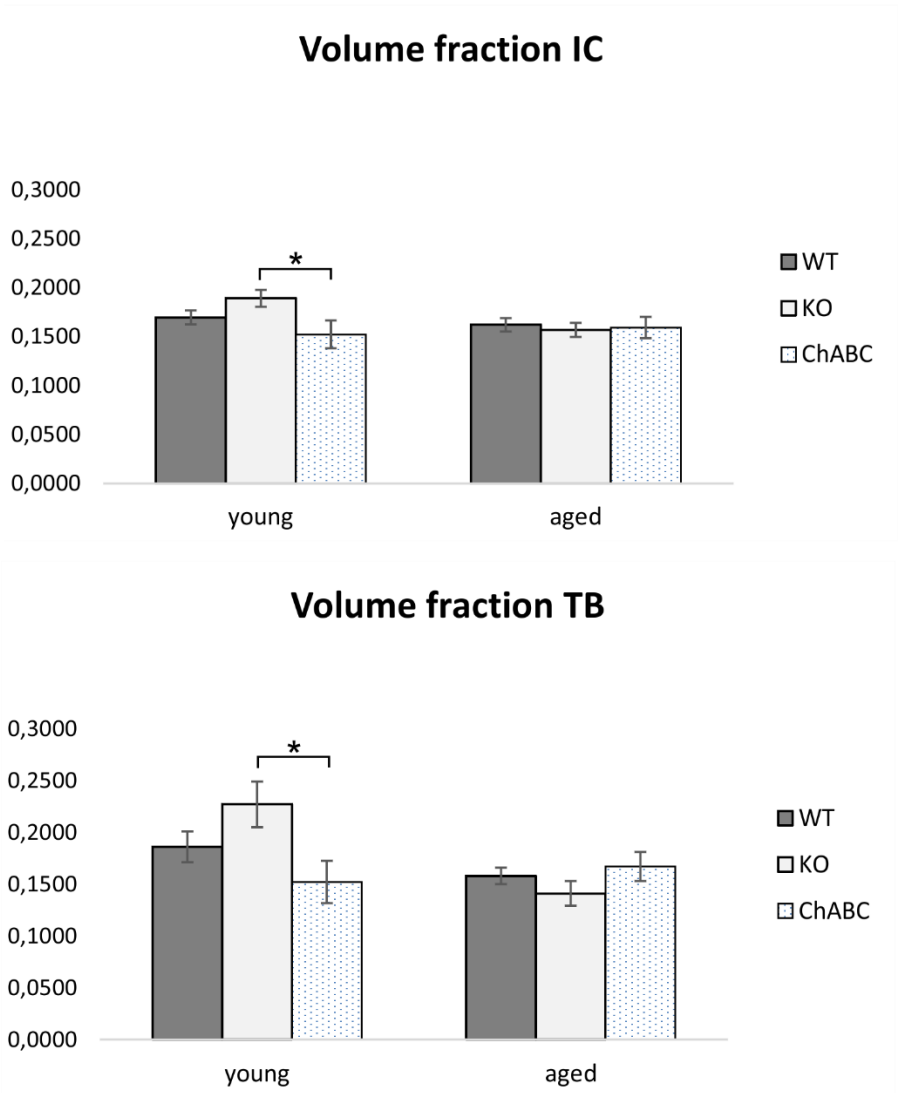

Figure 24: Mean ECS volume fraction measured using the RTI method. The mean values of the ECS volume fraction in the inferior colliculus (IC) and the trapezoid body (TB) of the wild type (WT), Bral2-deficient mice (KO) and chondroitinase ABC (chABC) treated animals. * marks a significant difference between the KO and chABC treated animals. Data are given as mean ± SEM. P values under 0.05 were considered statistically significant (*; $P \leq 0.05$). SEM - standard error of the mean

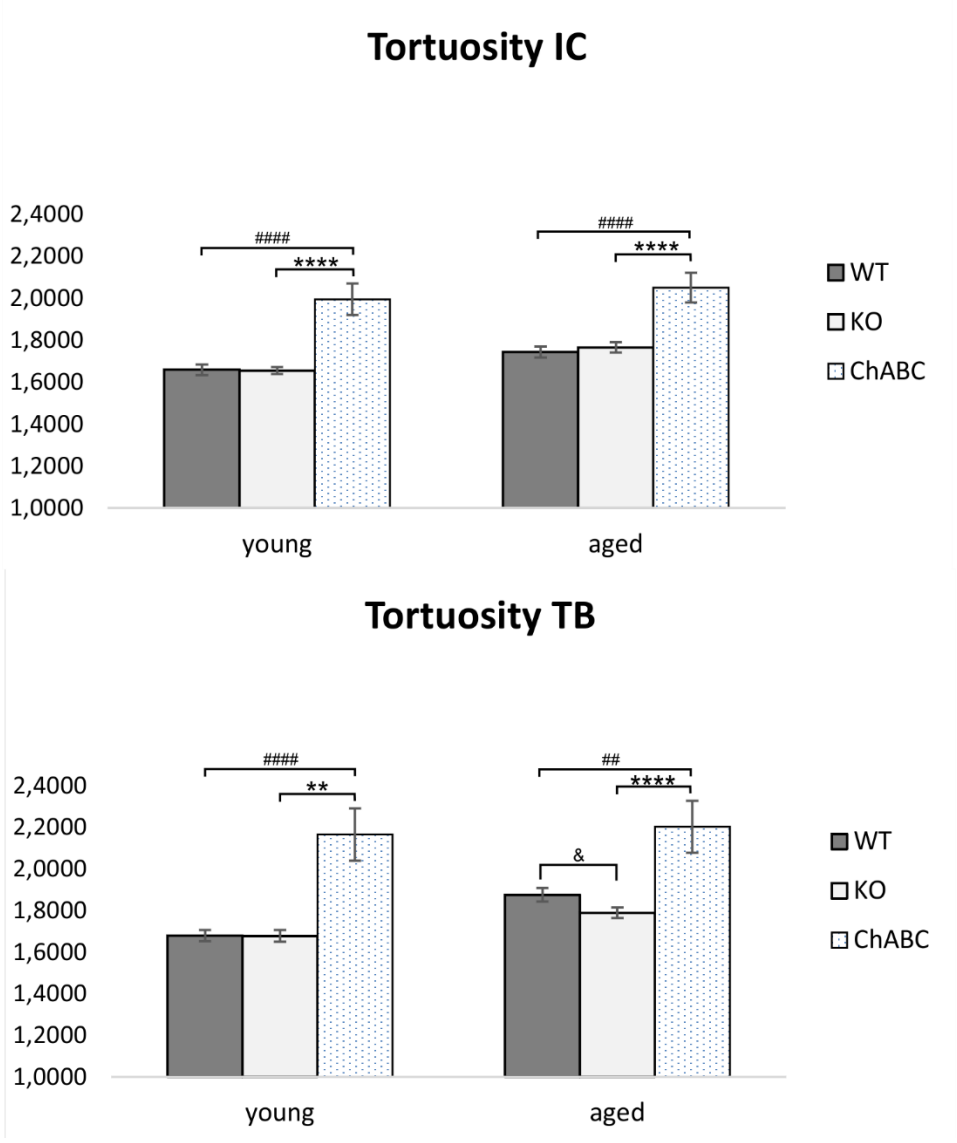

Figure 25: Comparison of the mean values of the tortuosity. The mean values of tortuosity in the inferior colliculus (IC) and trapezoid body (TB) of the wild type (WT), Bral2-deficient mice (KO) and chondroitinase ABC (chABC) treated animals. * marks a significant difference between the KO and chABC treated animal, # marks a significance between the WT and chABC treated mice, & marks a significant change between the WT and KO mice. Data are given as mean ± SEM. P values under 0.05 were considered statistically significant (#; $P \leq 0.05$). P values under 0.01 were considered very statistically significant (**, $P \leq 0.01$). P values under 0.0001 were considered extremely statistically significant (**** or ####, $P \leq 0.0001$). SEM - standard error of the mean

7.5 Expression of the *Wisteria floribunda* agglutinin after administration of the chondroitinase ABC

To confirm the disruption of the PNNs in the chABC treated tissue, we stained the slices with *Wisteria floribunda* agglutinin. In the WT animals, WFA stains the ECM molecules and the PNNs. After chABC enzymatically cut the ECM molecules and the binding sites for WFA disappear,the WFA staining was abolished (Fig. 26).

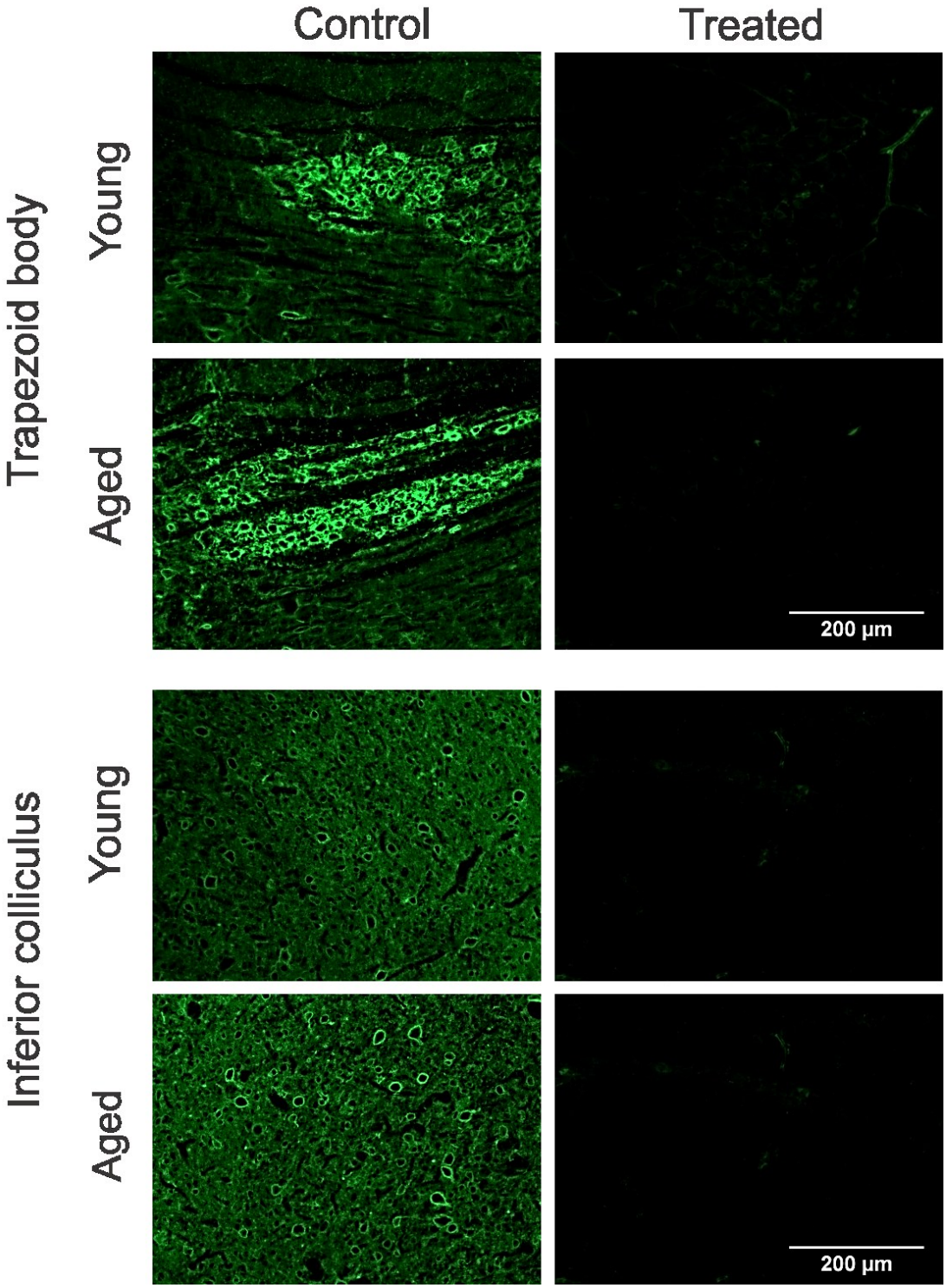

Figure 26: Wisteria floribunda agglutinin (WFA) staining. Application of the chondroitinase ABC (chABC) resulted in the disruption of the perineuronal nets. Scale is depicted in the image and is the same in the inferior colliculus and trapezoid body. "Treated" referes to the tissue after the incubation with chABC.

8. Discussion

Bral2 deficiency

Link proteins are stabilizing the hyaluronan-lectican binding in the PNNs. Since the Bral2 LP has analogous role as Bral1 (Oohashi et al. 2002) in the white matter, than its absence could lead to similar physiological changes. Disruption of the perinodal nets in the adult Bral1-deficient mice led to a decrease in tortuosity in all axes of anisotropic corpus callosum, while no significant changes in the ECS volume fraction were observed (Bekku et al. 2010). In this study, we did not observed any significant changes in the ECS volume fraction or tortuosity between young the WT and KO mice in the TB. No difference of the ECS diffusion parameters from their control values was detected either in the IC of the KO mice. This region is devoid of Bral2 expression and it was set as a negative control. The PNNs based on aggrecan and Crtl1 LP, which often co-localize (Bekku et al. 2012; Galtrey et al. 2008), were presented in the both regions of interests and were not affected by Bral2 deletion. These Crtl1-aggrecan based PNNs were overall much more prominent than the Bral2-brevican based PNNs in the TB. Therefore, after disappearance of Bral2-based PNNs, the neurons are still ensheathed and the normal physiology may not be altered. Additionally, the deletion of Bral2 LP could be partially compensated by Crtl1 LP. As the brevican, which often co-localize with Bral2 LP (Bekku et al. 2003), is still present in the TB of the KO mice and maintains the PNN pattern, we could assume that it is possible, however, immunohistochemical staining have shown only slight and non-significant increase in the expression of Crtl1 LP. The mentioned compensation could not occur in the perinodal nets as Bral1 LP is the only LP in this ECM assembly (Oohashi et al. 2002) leading to apparent changes in the ECM assembly already in the young animals.

The PNNs contain a large amount of fixed negative binding sites (Morawski et al. 2015), which may either bind water or positively charged ions and thus maintain the ECS volume and create diffusion barriers for cations. The disruption of the PNNs in mice mutant for TN-R, TN-C (Syková et al. 2005) resulted in a decrease in the ECS volume fraction and tortuosity. However, tenascins are core proteins of the ECM their deletion lead to a total disruption of the PNN assembly (Morawski et al. 2014). In the present study using the Bral2-deficient mice, no such changes did occur as tenascin and all lecticans (including brevican) do not disappear from the ECS and the ECM complexes based on Crtl1 and aggrecan are fully preserved.

Aging

The fact that Bral2 deletion led to alterations in the ECS diffusion parameters only in the aged mice TB, suggests that age should be taken into account when interpreting the effect of an ECM protein deficiency. We discovered a significant increase in tortuosity during aging in all studied groups and a decrease in the ECS volume fraction in the both regions of interest in the KO mice. The decrease in the ECS volume fraction and increase in tortuosity with an increasing age seems to be a common feature of the developing and aging brain (Syková and Nicholson 2008; Syková, Mazel, and Šimonová 1998). Other studies using the RTI method showed a decrease in α in the cortex together with hippocampus and corpus calosum during development and aging (Lehmenkühler et al. 1993; Syková et al. 2002). However, the relation between the ECS volume fraction and age is complex and many quantitative and qualitative changes in the ECM composition, changes in cell numbers and morphology, myelination and demyelination or protective mechanisms can play a role. In the current study, we have discovered the age related decrease in the ECS volume fraction in the both regions of interest between young and aged KO mice only and not in the WT animals. In the trapezoid body, the absence of Bral2 LP and related disruption of Bral2-based PNNs could lead to higher susceptibility and age-related loss of synapses, neuronal degeneration, astrogliosis and alterations in the ECM composition resulting in the alterations in the ECS diffusion parameters during aging. Some change in the extracellular diffusion could occur even in the IC as a result of overall changed expression of proteins in the knockout animal brain.

Besides the ECM, changes in the astroglia morphology and especially its processes represent another important source of the additional diffusion barriers affecting tortuosity. Surface area of the GFAP positive astrocytes mostly increased during ageing. However, this increase was less pronounced in the TB of the KO animals than that of WT mice. In the same structure, the width of the GFAP positive processes markedly increased during ageing in the KO mice but not in the WT animals. As these changes were not observed in the IC (negative control) we could assume that the changes are induced by the indirect effect of the Bral2 deficiency on the PNN-related neuroprotection and higher susceptibility of the Bral2 negative tissue to the age-related changes. The TB contains much more GFAP positive cells than IC and the role of astrocytes in the vicinity of the calyx of Held is highly studied matter (Reyes-Haro et al. 2010). However, the staining only for GFAP protein, a marker of reactive astrocytes,

cannot fully reflect the overall behavior of astrocytes in the KO mice as it does not stain the fine secondary and tertiary processes, which changes might highly influence the tortuosity values. Effect of astrocytes on physiological aging is generally unknown (Rodríguez-Arellano et al. 2016; Gómez-Gonzalo et al. 2017). Astrocyte activation is usually seen to have beneficial aspects from limiting lesion size after trauma to active neuroprotection, however, reactive gliosis can exert inhibitory effects on neuroplasticity and CNS regeneration (Pekny, Wilhelmsson, and Pekna 2014; Steele and Robinson 2012).

Our results suggest that aging is a critical point revealing the effect of Bral2 deficiency on the ECS diffusion in the medial nucleus of the trapezoid body. This might be due to either enhanced age-related damage of neurons lacking protective PNNs or a different molecular assembly in young and aged tissue. Alterations in the ECS diffusion parameters may in turn affect the diffusion of neuroactive substances, and thus extrasynaptic as well as synaptic transmission. Nevertheless, further studies are needed to clarify the mechanisms of the ECM remodeling in the young and old brain.

Enzymatic disruption of PNNs

The presence of PNNs has neuroprotective effect (Suttkus et al. 2012) and act as a buffer system for cations at synapses and nodes of Ranvier's enabling faster signal transmission (Bekku et al. 2010; Blosa et al. 2015). We investigated whether the PNN decomposition, which is observed in the link protein deficient animals (Bekku et al. 2010) has a similar impact on the diffusion through ECS as enzymatic disruption of the PNNs by chABC. Our results indicate that the effect of the ECM enzymatic treatment is completely different from that of Bral2 deficiency, where the ECM is preserved and only its organization is changed. As PNNs possess high anionic binding sites it was shown that their disruption leads to the increased diffusion coefficient for bivalent calcium (Hrabetová et al. 2009) after the diffusion barriers and binding sites diminish after administration of chABC. In the case of small monovalent molecule TMA^+, the authors detected no change in tortuosity in the cortex and a slight but insignificant tendency to the tortuosity increase in the hippocampus (Hrabetová et al. 2009), suggesting that the effect of chABC on tortuosity changes might be region-dependent. In our study, we observed a significantly increased value of tortuosity after treatment, which may be caused by the presence of smaller but plenty obstacles arising from the enzymatic splitting of the ECM

macromolecules to a smaller molecules, which might be due to the different tissue organization of the TB more concentrated as in the cortex and hippocampus (Hrabetová et al. 2009) and could significantly hinder the diffusion of TMA^+.

9. Conclusion

Our results suggest that the ECM in the IC and TB are based on the different molecules as Bral2-brevican based PNNs are present only in the TB, unlike the Crtl1-aggrecan based PNNs that were observed in both nuclei. Bral2 deficiency-induced decrease in tortuosity in the TB is age related as it was not observed between the WT and KO mice in the young animals. In the KO mice, Bral2 LP staining diminish, while the expression of brevican, which often co-localize with the Bral2, is not changed, suggesting the reorganization of the ECM assembly in the KO animals. From our findings, it is evident that aging is necessary to reveal the effect of the Bral2 deletion on the ECS diffusion properties. It is plausible that this effect is indirect and may be related to the different ECM assembly in the young and aged animals or to the impaired neuroprotection and higher sensitivity to the age-associated alteration in the Bral2-deficient tissue including astrogliosis-like rebuilding. As Bral2 often co-localized with brevican, which was shown to maintain fast synaptic transmission at the calyx of Held in the TB (Blosa et al. 2015), it is possible that Bral2 deficiency and associated extracellular diffusion alterations could affect hearing functions. However, the role of Bral2 protein is far from being fully elucidated and is worthy of further research.

Due to their role in the synaptic plasticity, learning or neuroprotection, enzymatic regulations of the PNNs are intensively studied (Kwok et al. 2011; Fawcett 2015). However, a discrepancy between our results and previous findings (Hrabetová et al. 2009) indicate that effect of the enzymatic treatment might not be predictable easily and can vary in the different structures.

References

Adams, I., K. Brauer, C. Arélin, W. Härtig, A. Fine, M. Mäder, T. Arendt, and G. Brückner. 2001. "Perineuronal Nets in the Rhesus Monkey and Human Basal Forebrain Including Basal Ganglia." *Neuroscience* 108 (2): 285–98. doi:10.1016/S0306-4522(01)00419-5.

Agnati, L. F., G. Leo, A. Zanardi, S. Genedani, A. Rivera, K. Fuxe, and D. Guidolin. 2006. "Volume Transmission and Wiring Transmission from Cellular to Molecular Networks: History and Perspectives." *Acta Physiologica* 187 (1–2): 329–44. doi:10.1111/j.1748-1716.2006.01579.x.

Allen Institute for Brain Science. 2011. "Allen Mouse Brain Atlas." http://mouse.brain-map.org/.

Alpár, A., U. Gärtner, W. Härtig, and G. Brückner. 2006. "Distribution of Pyramidal Cells Associated with Perineuronal Nets in the Neocortex of Rat." *Brain Research* 1120 (1): 13–22. doi:10.1016/j.brainres.2006.08.069.

Araque, A., V. Parpura, R. P. Sanzgiri, and P. G. Haydon. 1999. "Tripartite Synapses: Glia, the Unacknowledged Partner." *Trends in Neurosciences* 22 (5): 208–15. doi:10.1016/S0166-2236(98)01349-6.

Arranz, A. M., K. L. Perkins, F. Irie, D. P. Lewis, J. Hrabe, F. Xiao, N. Itano, K. Kimata, S. Hrabetova, and Y. Yamaguchi. 2014. "Hyaluronan Deficiency Due to Has3 Knock-Out Causes Altered Neuronal Activity and Seizures via Reduction in Brain Extracellular Space." *Journal of Neuroscience* 34 (18): 6164–76. doi:10.1523/JNEUROSCI.3458-13.2014.

Asher, R. A., R. J. Scheibe, H. D. Keiser, and A. Bignami. 1995. "On the Existence of a Cartilage-like Proteoglycan and Link Proteins in the Central Nervous System." *Glia* 13 (4): 294–308. doi:10.1002/glia.440130406.

Aspberg, A. 2016. "Cartilage Proteoglycans." In *Cartilage: Volume 1: Physiology and Development*, edited by Susanne Grässel and Attila Aszódi, 1–22. Cham: Springer International Publishing. doi:10.1007/978-3-319-29568-8_1.

Aspberg, A., R. Miura, S. Bourdoulous, M. Shimonaka, D. Heinegârd, M. Schachner, E. Ruoslahti, and Y. Yamaguchi. 1997. "The C-Type Lectin Domains of Lecticans, a Family of Aggregating Chondroitin Sulfate Proteoglycans, Bind Tenascin-R by Protein-Protein Interactions Independent of Carbohydrate Moiety." *Proceedings of the National Academy of Sciences of the United States of America* 94 (19): 10116–21. doi:10.1073/pnas.94.19.10116.

Asztely, F., G. Erdemli, and D. M. Kullmann. 1997. "Extrasynaptic Glutamate Spillover in the Hippocampus: Dependence on Temperature and the Role of Active Glutamate Uptake." *Neuron* 18 (2): 281–93. doi:10.1016/S0896-6273(00)80268-8.

Balmer, T. S., V. M. Carels, J. L. Frisch, and T. A. Nick. 2009. "Modulation of Perineuronal Nets and Parvalbumin with Developmental Song Learning." *The Journal of Neuroscience : The Official Journal of the Society for Neuroscience* 29 (41): 12878–85. doi:10.1523/JNEUROSCI.2974-09.2009.

Bekku, Y., and T. Oohashi. 2010. "Neurocan Contributes to the Molecular Heterogeneity of the Perinodal ECM." *Archives of Histology and Cytology* 73 (2): 95–102. doi:10.1679/aohc.73.95.

Bekku, Y., U. Rauch, Y. Ninomiya, and T. Oohashi. 2009. "Brevican Distinctively Assembles Extracellular Components at the Large Diameter Nodes of Ranvier in the CNS." *Journal of Neurochemistry* 108 (5): 1266–76. doi:10.1111/j.1471-

4159.2009.05873.x.
Bekku, Y., M. Saito, M. Moser, M. Fuchigami, A. Maehara, M. Nakayama, S. Kusachi, Y. Ninomiya, and T. Oohashi. 2012. “Bral2 Is Indispensable for the Proper Localization of Brevican and the Structural Integrity of the Perineuronal Net in the Brainstem and Cerebellum.” *The Journal of Comparative Neurology* 520 (8): 1721–36. doi:10.1002/cne.23009.
Bekku, Y., W.-D. Su, S. Hirakawa, R. Fässler, A. Ohtsuka, J. S. Kang, J. Sanders, T. Murakami, Y. Ninomiya, and T. Oohashi. 2003. “Molecular Cloning of Bral2, a Novel Brain-Specific Link Protein, and Immunohistochemical Colocalization with Brevican in Perineuronal Nets☆.” *Molecular and Cellular Neuroscience* 24 (1): 148–59. doi:10.1016/S1044-7431(03)00133-7.
Bekku, Y., L. Vargová, Y. Goto, I. Vorísek, L. Dmytrenko, M. Narasaki, A. Ohtsuka, et al. 2010. “Bral1: Its Role in Diffusion Barrier Formation and Conduction Velocity in the CNS.” *The Journal of Neuroscience : The Official Journal of the Society for Neuroscience* 30 (8): 3113–23. doi:10.1523/JNEUROSCI.5598-09.2010.
Bertolotto, A., E. Manzardo, and R. Guglielmone. 1996. “Immunohistochemical Mapping of Perineuronal Nets Containing Chondroitin Unsulfate Proteoglycan in the Rat Central Nervous System.” *Cell and Tissue Research* 283 (2): 283–95. doi:10.1007/s004410050538.
Bertolotto, A, G Rocca, G Canavese, A Migheli, and D Schiffer. 1991. “Chondroitin Sulfate Proteoglycan Surrounds a Subset of Human and Rat CNS Neurons.” *Journal of Neuroscience Research* 29 (2): 225–34.
Beurdeley, M., J. Spatazza, H. H. C. Lee, S. Sugiyama, C. Bernard, a. a. Di Nardo, T. K. Hensch, and a. Prochiantz. 2012. “Otx2 Binding to Perineuronal Nets Persistently Regulates Plasticity in the Mature Visual Cortex.” *Journal of Neuroscience* 32 (27): 9429–37. doi:10.1523/JNEUROSCI.0394-12.2012.
Blosa, M., M. Sonntag, G. Brückner, C. Jäger, G. Seeger, R. T. Matthews, R. Rübsamen, T. Arendt, and M. Morawski. 2013. “Unique Features of Extracellular Matrix in the Mouse Medial Nucleus of Trapezoid Body - Implications for Physiological Functions.” *Neuroscience* 228: 215–34. doi:10.1016/j.neuroscience.2012.10.003.
Blosa, M., M. Sonntag, C. Jäger, S. Weigel, J. Seeger, R. Frischknecht, C. I. Seidenbecher, et al. 2015. “The Extracellular Matrix Molecule Brevican Is an Integral Component of the Machinery Mediating Fast Synaptic Transmission at the Calyx of Held.” *The Journal of Physiology* 593 (19): 4341–60. doi:10.1113/JP270849.
Blue, M E, and J G Parnavelas. 1983. “The Formation and Maturation of Synapses in the Visual Cortex of the Rat. II. Quantitative Analysis.” *Journal of Neurocytology* 12 (4): 697–712. http://www.ncbi.nlm.nih.gov/pubmed/6619907.
Bozdagi, O., V. Nagy, K. T. Kwei, and G. W. Huntley. 2007. “In Vivo Roles for Matrix Metalloproteinase-9 in Mature Hippocampal Synaptic Physiology and Plasticity.” *Journal of Neurophysiology* 98 (1): 334–44. doi:10.1152/jn.00202.2007.
Brakebusch, C., C. I. Seidenbecher, U. Rauch, H. Matthies, H. Meyer, M. Krug, T. M. Böckers, et al. 2002. “Brevican-Deficient Mice Display Impaired Hippocampal CA1 Long-Term Potentiation but Show No Obvious Deficits in Learning and Memory.” *Molecular and Cellular Biology* 22 (21): 7417–27. doi:10.1128/MCB.22.21.7417.
Brauer, K., G. Bruckner, L. Leibnitz, and L. Werner. 1984. “Structural and Cytochemical Features of Perineuronal Glial Nets in the Rat Brain.” *Acta Histochemica* 74 (1): 53–60.

doi:10.1016/S0065-1281(84)80026-4.
Brückner, G., K. Brauer, W. Härtig, J. R. Wolff, M. J. Rickmann, A. Derouiche, B. Delpech, N. Girard, W. H. Oertel, and A. Reichenbach. 1993. “Perineuronal Nets Provide a Polyanionic, Glia-Associated Form of Microenvironment around Certain Neurons in Many Parts of the Rat Brain.” *Glia* 8 (3): 183–200. doi:10.1002/glia.440080306.
Brückner, G., J. Grosche, S. Schmidt, W. Härtig, R. U. Margolis, B. Delpech, C. I. Seidenbecher, R. Czaniera, and M. Schachner. 2000. “Postnatal Development of Perineuronal Nets in Wild-Type Mice and in a Mutant Deficient in Tenascin-R.” *Journal of Comparative Neurology* 428 (4): 616–29. doi:10.1002/1096-9861(20001225)428:4<616::AID-CNE3>3.0.CO;2-K.
Brückner, G., W. Härtig, J. Kacza, J. Seeger, K. Welt, and K. Brauer. 1996. “Extracellular Matrix Organization in Various Regions of Rat Brain Grey Matter.” *Journal of Neurocytology* 25 (5): 333–46. http://www.ncbi.nlm.nih.gov/pubmed/8818977.
Brückner, G., D. Hausen, W. Härtig, M. Drlicek, T. Arendt, and K. Brauer. 1999. “Cortical Areas Abundant in Extracellular Matrix Chondroitin Sulphate Proteoglycans Are Less Affected by Cytoskeletal Changes in Alzheimer’s Disease.” *Neuroscience* 92 (3): 791–805. doi:10.1016/S0306-4522(99)00071-8.
Brückner, G., M. Morawski, and T. Arendt. 2008. “Aggrecan-Based Extracellular Matrix Is an Integral Part of the Human Basal Ganglia Circuit.” *Neuroscience* 151 (2): 489–504. doi:10.1016/j.neuroscience.2007.10.033.
Brückner, G., G. Seeger, K. Brauer, W. Härtig, J. Kacza, and V. Bigl. 1994. “Cortical Areas Are Revealed by Distribution Patterns of Proteoglycan Components and Parvalbumin in the Mongolian Gerbil and Rat.” *Brain Research* 658 (1–2): 67–86. doi:10.1016/S0006-8993(09)90012-9.
Brückner, G., S. Szeöke, S. Pavlica, J. Grosche, and J. Kacza. 2006. “Axon Initial Segment Ensheathed by Extracellular Matrix in Perineuronal Nets.” *Neuroscience* 138 (2): 365–75. doi:10.1016/j.neuroscience.2005.11.068.
Cabungcal, Jan-Harry, Pascal Steullet, Hirofumi Morishita, Rudolf Kraftsik, Michel Cuenod, Takao K Hensch, and Kim Q Do. 2013. “Perineuronal Nets Protect Fast-Spiking Interneurons against Oxidative Stress.” *Proceedings of the National Academy of Sciences of the United States of America* 110 (22): 9130–35. doi:10.1073/pnas.1300454110.
Carulli, D., T. Pizzorusso, J. C. F. Kwok, E. Putignano, A. Poli, S. Forostyak, M. R. Andrews, S. S. Deepa, T. T. Glant, and J. W. Fawcett. 2010. “Animals Lacking Link Protein Have Attenuated Perineuronal Nets and Persistent Plasticity.” *Brain : A Journal of Neurology* 133 (Pt 8): 2331–47. doi:10.1093/brain/awq145.
Carulli, D., K. E. Rhodes, D. J. Brown, T. P. Bonnert, S. J. Pollack, K. Oliver, P. Strata, and J. W. Fawcett. 2006. “Composition of Perineuronal Nets in the Adult Rat Cerebellum and the Cellular Origin of Their Components.” *The Journal of Comparative Neurology* 494 (4): 559–77. doi:10.1002/cne.20822.
Carulli, D., K. E. Rhodes, and J. W. Fawcett. 2007. “Upregulation of Aggrecan, Link Protein 1, and Hyaluronan Synthases during Formation of Perineuronal Nets in the Rat Cerebellum.” *J Comp Neurol* 501 (1): 83–94. doi:10.1002/cne.
Celio, M. R. 1986. “Parvalbumin in Most Gamma-Aminobutyric Acid-Containing Neurons of the Rat Cerebral Cortex.” *Science* 231 (4741): 995–97.
Celio, M. R., and R. Chiquet-Ehrismann. 1993. “‘Perineuronal Nets’ around Cortical

Interneurons Expressing Parvalbumin Are Rich in Tenascin." *Neuroscience Letters* 162 (1–2): 137–40. doi:10.1016/0304-3940(93)90579-A.
Cicanic, M., M. Edamatsu, Y. Bekku, I. Voříšek, T. Oohashi, and L. Vargová. Submitted. "A Deficiency of the Link Protein Bral2 Affects the Size of the Extracellular Space in the Thalamus of Aged Mice." *Journal of Neuroscience Research*.
Cicanic, M., E. Sykova, and L. Vargova. 2012. "Bral1: 'Superglue' for the Extracellular Matrix in the Brain White Matter." *International Journal of Biochemistry and Cell Biology* 44 (4). Elsevier Ltd: 596–99. doi:10.1016/j.biocel.2012.01.009.
Deepa, S. S., D. Carulli, C. Galtrey, K. Rhodes, J. Fukuda, T. Mikami, K. Sugahara, and J. W. Fawcett. 2006. "Composition of Perineuronal Net Extracellular Matrix in Rat Brain." *Journal of Biological Chemistry* 281 (26): 17789–800. doi:10.1074/jbc.M600544200.
Dityatev, A., and T. Fellin. 2008. "Extracellular Matrix in Plasticity and Epileptogenesis." *Neuron Glia Biology* 4 (3): 235–47. doi:10.1017/S1740925X09000118.
Dityatev, A., and D. A. Rusakov. 2011. "Molecular Signals of Plasticity at the Tetrapartite Synapse." *Current Opinion in Neurobiology* 21 (2): 353–59. doi:10.1016/j.conb.2010.12.006.
Dityatev, A., and M. Schachner. 2006. "The Extracellular Matrix and Synapses." *Cell and Tissue Research* 326 (2): 647–54. doi:10.1007/s00441-006-0217-1.
Du, J., L. Zhang, M. Weiser, B. Rudy, and C. J. McBain. 1996. "Developmental Expression and Functional Characterization of the Potassium-Channel Subunit Kv3.1b in Parvalbumin-Containing Interneurons of the Rat Hippocampus." *The Journal of Neuroscience* 16 (2): 506–18.
Fader, S., K. Imaizumi, Y. Yanagawa, and Ch. Lee. 2016. "Wisteria Floribunda Agglutinin-Labeled Perineuronal Nets in the Mouse Inferior Colliculus, Thalamic Reticular Nucleus and Auditory Cortex." *Brain Sciences* 6 (2): 13. doi:10.3390/brainsci6020013.
Fawcett, J. W. 2015. *The Extracellular Matrix in Plasticity and Regeneration after CNS Injury and Neurodegenerative Disease*. *Progress in Brain Research*. 1sted. Vol. 218. Elsevier B.V. doi:10.1016/bs.pbr.2015.02.001.
Fayuk, D., P. G. Aitken, G. G. Somjen, and D. A. Turner. 2002. "Two Different Mechanisms Underlie Reversible, Intrinsic Optical Signals in Rat Hippocampal Slices." *Journal of Neurophysiology* 87 (4): 1924–37. doi:10.1152/jn.00231.2001.
Fenstermacher, J., and T. Kaye. 1988. "Drug ' Diffusion ' within the Brain." *Annals of the New York Academy of Sciences* 531: 29–39.
Foster, N. L., J. G. Mellott, and B. R. Schofield. 2014. "Perineuronal Nets and GABAergic Cells in the Inferior Colliculus of Guinea Pigs." *Frontiers in Neuroanatomy* 7 (January): 53. doi:10.3389/fnana.2013.00053.
Frischknecht, R., M. Heine, D. Perrais, C. I. Seidenbecher, D. Choquet, and E. D. Gundelfinger. 2009. "Brain Extracellular Matrix Affects AMPA Receptor Lateral Mobility and Short-Term Synaptic Plasticity." *Nature Neuroscience* 12 (7): 897–904. doi:10.1038/nn.2338.
Galtrey, C. M., and J. W. Fawcett. 2007. "The Role of Chondroitin Sulfate Proteoglycans in Regeneration and Plasticity in the Central Nervous System." *Brain Research Reviews* 54 (1): 1–18. doi:10.1016/j.brainresrev.2006.09.006.
Galtrey, C. M., J. C. F. Kwok, D. Carulli, K. E. Rhodes, and J. W. Fawcett. 2008. "Distribution and Synthesis of Extracellular Matrix Proteoglycans, Hyaluronan, Link

Proteins and Tenascin-R in the Rat Spinal Cord." *European Journal of Neuroscience* 27: 1373–90. doi:10.1111/j.1460-9568.2008.06108.x.
García-Alías, G., S. Barkhuysen, M. Buckle, and J. W. Fawcett. 2009. "Chondroitinase ABC Treatment Opens a Window of Opportunity for Task-Specific Rehabilitation." *Nature Neuroscience* 12 (9): 1145–51. doi:10.1038/nn.2377.
Geissler, M., C. Gottschling, a. Aguado, U. Rauch, C. H. Wetzel, H. Hatt, and a. Faissner. 2013. "Primary Hippocampal Neurons, Which Lack Four Crucial Extracellular Matrix Molecules, Display Abnormalities of Synaptic Structure and Function and Severe Deficits in Perineuronal Net Formation." *Journal of Neuroscience* 33 (18): 7742–55. doi:10.1523/JNEUROSCI.3275-12.2013.
Gogolla, N., P. Caroni, A. Luthi, and C. Herry. 2009. "Perineuronal Nets Protect Fear Memories from Erasure." *Science* 325 (5945): 1258–61. doi:10.1126/science.1174146.
Gómez-Gonzalo, M., M. Martin-Fernandez, R. Martínez-Murillo, S. Mederos, A. Hernández-Vivanco, S. Jamison, A. P. Fernandez, et al. 2017. "Neuron-Astrocyte Signaling Is Preserved in the Aging Brain." *Glia* 65 (4): 569–80. doi:10.1002/glia.23112.
Hagihara, K., R. Miura, R. Kosaki, E. Berglund, B. Ranscht, and Y. Yamaguchi. 1999. "Immunohistochemical Evidence for the Brevican-Tenascin-R Interaction: Colocalization in Perineuronal Nets Suggests a Physiological Role for the Interaction in the Adult Rat Brain." *Journal of Comparative Neurology* 410 (2): 256–64. doi:10.1002/(SICI)1096-9861(19990726)410:2<256::AID-CNE7>3.0.CO;2-5.
Hardingham, T. E. 1979. "The Role of Link-Protein in the Structure of Cartilage Proteoglycan Aggregates." *The Biochemical Journal* 177 (1): 237–47. http://www.pubmedcentral.nih.gov/articlerender.fcgi?artid=1186361&tool=pmcentrez&rendertype=abstract.
Härtig, W., A. Derouiche, K. Welt, K. Brauer, J. Grosche, M. Mäder, A. Reichenbach, and G. Brückner. 1999. "Cortical Neurons Immunoreactive for the Potassium Channel Kv3.1b Subunit Are Predominantly Surrounded by Perineuronal Nets Presumed as a Buffering System for Cations." *Brain Research* 842 (1): 15–29. doi:10.1016/S0006-8993(99)01784-9.
Härtig, W., A. Singer, J. Grosche, K. Brauer, O. P. Ottersen, and G. Brückner. 2001. "Perineuronal Nets in the Rat Medial Nucleus of the Trapezoid Body Surround Neurons Immunoreactive for Various Amino Acids, Calcium-Binding Proteins and the Potassium Channel Subunit Kv3.1b." *Brain Research* 899 (1–2): 123–33. doi:10.1016/S0006-8993(01)02211-9.
Härtig, Wolfgang, Kurt Brauer, and Gert Brückner. 1992. "Wisteria Floribunda Agglutinin-Labelled Nets Surround Parvalbumin-Containing Neurons." *Neuroreport* 3 (10): 869–72.
Hendry, S. H., E. G. Jones, S. Hockfield, and R. D. McKay. 1988. "Neuronal Populations Stained with the Monoclonal Antibody Cat-301 in the Mammalian Cerebral Cortex and Thalamus." *The Journal of Neuroscience : The Official Journal of the Society for Neuroscience* 8 (2): 518–42.
Hilbig, H., S. Nowack, K. Boeckler, H. J. Bidmon, and K. Zilles. 2007. "Characterization of Neuronal Subsets Surrounded by Perineuronal Nets in the Rhesus Auditory Brainstem." *Journal of Anatomy* 210 (5): 507–17. doi:10.1111/j.1469-7580.2007.00713.x.
Hrabetová, S., D. Masri, L. Tao, F. Xiao, and Ch. Nicholson. 2009. "Calcium Diffusion Enhanced after Cleavage of Negatively Charged Components of Brain Extracellular

Matrix by Chondroitinase ABC." *The Journal of Physiology* 587 (Pt 16): 4029–49. doi:10.1113/jphysiol.2009.170092.
Chen, K. C., and C. Nicholson. 2000. "Changes in Brain Cell Shape Create Residual Extracellular Space Volume and Explain Tortuosity Behavior during Osmotic Challenge." *Proceedings of the National Academy of Sciences of the United States of America* 97 (15): 8306–11. doi:10.1073/pnas.150338197.
Chen, W., Y. S. Li, J. Gao, X. Y. Lin, and X. H. Li. 2016. "AMPA Receptor Antagonist NBQX Decreased Seizures by Normalization of Perineuronal Nets." *PLoS ONE* 11 (11): 1–16. doi:10.1371/journal.pone.0166672.
Chvátal, A., T. Berger, I. Voříšek, R. K. Orkand, H. Kettenmann, and E. Syková. 1997. "Changes in Glial K+ Currents with Decreased Extracellular Volume in Developing Rat White Matter." *Journal of Neuroscience Research* 49 (1): 98–106. doi:10.1002/(SICI)1097-4547(19970701)49:1<98::AID-JNR11>3.0.CO;2-0.
Jones, F. S., and P. L. Jones. 2000. "The Tenascin Family of ECM Glycoproteins: Structure, Function, and Regulation during Embryonic Development and Tissue Remodeling." *Developmental Dynamics* 218 (2): 235–59. doi:10.1002/(SICI)1097-0177(200006)218:2<235::AID-DVDY2>3.0.CO;2-G.
Kalb, R. G., and S. Hockfield. 1990. "Induction of a Neuronal Proteoglycan by the NMDA Receptor in the Developing Spinal Cord." *Science* 250 (4978): 294–96. doi:10.1126/science.2145629.
Kawaguchi, Y., H. Katsumaru, T. Kosaka, C. W. Heizmann, and K. Hama. 1987. "Fast Spiking Cells in Rat Hippocampus (CA1 Region) Contain the Calcium-Binding Protein Parvalbumin." *Brain Research* 416 (2): 369–74. doi:10.1016/0006-8993(87)90921-8.
Kawaguchi, Y., and Y. Kubota. 1998. "Neurochemical Features and Synaptic Connections of Large Physiologically-Identified GABAergic Cells in the Rat Frontal Cortex." *Neuroscience* 85 (3): 677–701. doi:10.1016/S0306-4522(97)00685-4.
Köppe, G., G. Brückner, W. Härtig, B. Delpech, and V. Bigl. 1997. "Characterization of Proteoglycan-Containing Perineuronal Nets by Enzymatic Treatments of Rat Brain Sections." *Histochemical Journal* 29 (1): 11–20. doi:10.1023/A:1026408716522.
Kosaka, T., and C. W. Heizmann. 1989. "Selective Staining of a Population of Parvalbumin-Containing GABAergic Neurons in the Rat Cerebral Cortex by Lectins with Specific Affinity for Terminal N-Acetylgalactosamine." *Brain Research* 483 (1): 158–63. doi:10.1016/0006-8993(89)90048-6.
Kume-Kick, J., T. Mazel, I. Vorisek, S. Hrabětová, L. Tao, and Ch. Nicholson. 2002. "Independence of Extracellular Tortuosity and Volume Fraction during Osmotic Challenge in Rat Neocortex." *The Journal of Physiology* 542 (Pt 2): 515–27. doi:10.1113/jphysiol.2002.017541.
Kwok, J. C. F., G. Dick, D. Wang, and J. W. Fawcett. 2011. "Extracellular Matrix and Perineuronal Nets in CNS Repair." *Developmental Neurobiology* 71 (11): 1073–89. doi:10.1002/dneu.20974.
Lehmenkühler, A., E. Syková, J. Svoboda, K. Zilles, and Ch. Nicholson. 1993. "Space Parameters in the Rat During Postnatal Development Determined By." *Neuroscience* 55 (2): 339–51. doi:10.1016/0306-4522(93)90503-8.
Li, C.H., and P.K.S. Tam. 1998. "An Iterative Algorithm for Minimus Cross Entropy Tresholding." *Pattern Recognition Letters* 19 (8): 771–76.
Li, Y., Z.-X. Li, T. Jin, Z.-Y. Wang, and P. Zhao. 2017. "Tau Pathology Promotes the

Reorganization of the Extracellular Matrix and Inhibits the Formation of Perineuronal Nets by Regulating the Expression and the Distribution of Hyaluronic Acid Synthases." *Journal of Alzheimer's Disease*, 1–15. doi:10.3233/JAD-160804.

Lundbaek, J.A., and A. J. Hansen. 1992. "Brain Interstitial Volume Fraction and Tortuosity in Anoxia. Evaluation of the Ion-Selective Micro-Electrode Method." *Acta Physiologica Scandinavica* 146 (4): 473–84. doi:10.1111/j.1748-1716.1992.tb09449.x.

Lundell, A., A. I. Olin, M. Mörgelin, S. Al-Karadaghi, A Aspberg, and D. T. Logan. 2004. "Structural Basis for Interactions between Tenascins and Lectican C-Type Lectin Domains." *Structure* 12 (8): 1495–1506. doi:10.1016/j.str.2004.05.021.

Lüth, H. J., J. Fischer, and M. R. Celio. 1992. "Soybean Lectin Binding Neurons in the Visual Cortex of the Rat Contain Parvalbumin and Are Covered by Glial Nets." *Journal of Neurocytology* 21 (3): 211–21. doi:10.1007/BF01194979.

Lux, H. D., and E Neher. 1973. "The Equilibration Time Course of [K+]o in Cat Cortex." *ExperiBrain Res.* 17 (2): 190–205.

Massey, J. M. 2006. "Chondroitinase ABC Digestion of the Perineuronal Net Promotes Functional Collateral Sprouting in the Cuneate Nucleus after Cervical Spinal Cord Injury." *Journal of Neuroscience* 26 (16): 4406–14. doi:10.1523/JNEUROSCI.5467-05.2006.

Mauney, S. A., K. M. Athanas, H. Pantazopoulos, N. Shaskan, E. Passeri, S. Berretta, and T.-U. W. Woo. 2013. "Developmental Pattern of Perineuronal Nets in the Human Prefrontal Cortex and Their Deficit in Schizophrenia." *Biological Psychiatry* 74 (6): 427–35. doi:10.1016/j.biopsych.2013.05.007.Developmental.

Maurel, P., U. Rauch, M. Flad, R. K. Margolis, and R. U. Margolis. 1994. "Phosphacan, a Chondroitin Sulfate Proteoglycan of Brain That Interacts with Neurons and Neural Cell-Adhesion Molecules, Is an Extracellular Variant of a Receptor-Type Protein Tyrosine Phosphatase." *Proceedings of the National Academy of Sciences of the United States of America* 91 (7): 2512–16. doi:10.1073/pnas.91.7.2512.

Mazel, T., Z. Simonová, and E. Syková. 1998. "Diffusion Heterogeneity and Anisotropy in Rat Hippocampus." *Neuroreport* 9 (7): 1299–1304. doi:10.1097/00001756-199805110-00008.

Melching, L. I., and P. J. Roughley. 1985. "The Role of Link Protein in Mediating the Interaction between Hyaluronic Acid and Newly Secreted Proteoglycan Subunits from Adult Human Articular Cartilage." *Journal of Biological Chemistry* 260 (30): 16279–85.

Milev, P., H. Monnerie, S. Popp, and R. U. K. Margolis. 1998. "The Core Protein of the Chondroitin Sulfate Proteoglycan Phosphacan Is a High-Affinity Ligand of Fibroblast Growth Factor- 2 and Potentiates Its Mitogenic Activity." *J.Biol.Chem.* 273 (34): 21439–42. doi:10.1074/jbc.273.34.21439.

Moon, L. D., R. A. Asher, K. E. Rhodes, and J. W. Fawcett. 2001. "Regeneration of CNS Axons back to Their Target Following Treatment of Adult Rat Brain with Chondroitinase ABC." *Nature Neuroscience* 4 (5): 465–66. doi:10.1038/87415.

Morawski, M., A. Alpár, G. Brückner, A. Fiedler, C. Jäger, G. Gati, J. T. Stieler, and T. Arendt. 2009. "Chondroitin Sulfate Proteoglycan-Based Extracellular Matrix in Chicken (Gallus Domesticus) Brain." *Brain Research* 1275. Elsevier B.V.: 10–23. doi:10.1016/j.brainres.2009.02.046.

Morawski, M., M. K. Brückner, P. Riederer, G. Brückner, and T. Arendt. 2004.

"Perineuronal Nets Potentially Protect against Oxidative Stress." *Experimental Neurology* 188 (2): 309–15. doi:10.1016/j.expneurol.2004.04.017.
Morawski, M., A. Dityatev, M. Hartlage-Rübsamen, M. Blosa, M. Holzer, K. Flach, S. Pavlica, et al. 2014. "Tenascin-R Promotes Assembly of the Extracellular Matrix of Perineuronal Nets via Clustering of Aggrecan Tenascin-R Promotes Assembly of the Extracellular Matrix of Perineuronal Nets via Clustering of Aggrecan." *Philos Trans R Soc Lond B Biol Sci.* 369 (1654): 20140046.
Morawski, M., T. Reinert, W. Meyer-Klaucke, F. E. Wagner, W. Tröger, A. Reinert, C. Jäger, G. Brückner, and T. Arendt. 2015. "Ion Exchanger in the Brain: Quantitative Analysis of Perineuronally Fixed Anionic Binding Sites Suggests Diffusion Barriers with Ion Sorting Properties." *Scientific Reports* 5 (November 2014). Nature Publishing Group: 16471. doi:10.1038/srep16471.
Morris, N. P., and Z. Henderson. 2000. "Perineuronal Nets Ensheath Fast Spiking, Parvalbumin-Immunoreactive Neurons in the Medial Septum/diagonal Band Complex." *European Journal of Neuroscience* 12 (3): 828–38. doi:10.1046/j.1460-9568.2000.00970.x.
Murakami, T., A. Ohtsuka, and K. Ono. 1996. "Neurons with Perineuronal Sulfated Proteoglycans in the Mouse Brain and Spinal Cord: Their Distribution and Reactions to Lectin Vicia Villosa Agglutinin and Golgi's Silver Nitrate." *Arch Histol Cytol* 59 (3): 219–31. http://www.ncbi.nlm.nih.gov/entrez/query.fcgi?cmd=Retrieve&db=PubMed&dopt=Citation&list_uids=8874754.
Murakami, T., T. Taguchi, and A. Ohtsuka. 1993. "The Occurrence in the Human Brain of Neurons with Strongly Negative-Charged Proteoglycans." *Archives of Histology and Cytology* 56 (1): 23–26. doi:10.1679/aohc.56.23.
Nagy, V., O. Bozdagi, and G. W. Huntley. 2007. "The Extracellular Protease Matrix Metalloproteinase-9 Is Activated by Inhibitory Avoidance Learning and Required for Long-Term Memory." *Learning & Memory* 14 (10): 655–64. doi:10.1101/lm.678307.
Neher, E., and H. D. Lux. 1973. "Rapid Changes of Potassium Concentration at the Outer Surface of Exposed Single Neurons during Membrane Current Flow." *The Journal of General Physiology* 61 (3): 385–99. http://www.pubmedcentral.nih.gov/articlerender.fcgi?artid=2203454&tool=pmcentrez&rendertype=abstract.
Nicholson, C., and J. M. Phillips. 1981. "Ion Diffusion Modified by Tortuosity and Volume Fraction in the Extracellular Microenvironment of the Rat Cerebellum." *The Journal of Physiology* 321: 225–57.
Nicholson, C., and E. Syková. 1998. "Extracellular Space Structure Revealed by Diffusion Analysis." *Trends in Neurosciences* 21 (5): 207–15. http://www.ncbi.nlm.nih.gov/pubmed/9610885.
Nicholson, C., and L. Tao. 1993. "Hindered Diffusion of High Molecular Weight Compounds in Brain Extracellular Microenvironment Measured with Integrative Optical Imaging." *Biophysical Journal* 65 (6): 2277–90. doi:10.1016/S0006-3495(93)81324-9.
Nicholson, Ch. 1992. "Quantitative Analysis of Extracellular Space Using the Method of TMA+ Iontophoresis and the Issue of TMA+ Uptake." *Canadian Journal of Physiology and Pharmacology* 70 Suppl. CANADA: S314-22.
Nicholson, Ch. 1993. "Ion-Selective Microelectrodes and Diffusion Measurements as Tools

to Explore the Brain Cell Microenvironment." *Journal of Neuroscience Methods* 48 (3): 199–213. doi:10.1016/0165-0270(93)90092-6.

Oohashi, T., M. Edamatsu, Y. Bekku, and D. Carulli. 2015. "The Hyaluronan and Proteoglycan Link Proteins: Organizers of the Brain Extracellular Matrix and Key Molecules for Neuronal Function and Plasticity." *Experimental Neurology* 274 (Pt B). Elsevier Inc.: 134–44. doi:10.1016/j.expneurol.2015.09.010.

Oohashi, T., S. Hirakawa, Y. Bekku, U. Rauch, D. R. Zimmermann, W.-D. Su, A. Ohtsuka, T. Murakami, and Y. Ninomiya. 2002. "Bral1, a Brain-Specific Link Protein, Colocalizing with the Versican V2 Isoform at the Nodes of Ranvier in Developing and Adult Mouse Central Nervous Systems." *Molecular and Cellular Neurosciences* 19 (1): 43–57. doi:10.1006/mcne.2001.1061.

Pekny, M., U. Wilhelmsson, and M. Pekna. 2014. "The Dual Role of Astrocyte Activation and Reactive Gliosis." *Neuroscience Letters* 565. Elsevier Ireland Ltd: 30–38. doi:10.1016/j.neulet.2013.12.071.

Perea, G., and A. Araque. 2005. "Properties of Synaptically Evoked Astrocyte Calcium Signal Reveal Synaptic Information Processing by Astrocytes." *Journal of Neuroscience* 25 (9): 2192–2203. doi:10.1523/JNEUROSCI.3965-04.2005.

Piet, R., L. Vargová, E. Syková, D. A. Poulain, and S. H. R. Oliet. 2004. "Physiological Contribution of the Astrocytic Environment of Neurons to Intersynaptic Crosstalk." *Proceedings of the National Academy of Sciences of the United States of America* 101 (7): 2151–55. doi:10.1073/pnas.0308408100.

Pizzorusso, T., P. Medini, N. Berardi, S. Chierzi, J. W. Fawcett, and L. Maffei. 2002. "Reactivation of Ocular Dominance Plasticity in the Adult Visual Cortex." *Science* 298 (5596): 1248–51. doi:10.1126/science.1072699.

Prokopová, S., L. Vargová, and E. Syková. 1997. "Heterogeneous and Anisotropic Diffusion in the Developing Rat Spinal Cord." *Neuroreport* 8 (16): 3527–32.

Rankin-Gee, E. K., P. A. McRae, E. Baranov, S. Rogers, L. Wandrey, and B. E. Porter. 2015. "Perineuronal Net Degradation in Epilepsy." *Epilepsia* 56 (7): 1124–33. doi:10.1111/epi.13026.

Reimers, S., M. Hartlage-Rübsamen, G. Brückner, and S. Roßner. 2007. "Formation of Perineuronal Nets in Organotypic Mouse Brain Slice Cultures Is Independent of Neuronal Glutamatergic Activity." *European Journal of Neuroscience* 25 (9): 2640–48. doi:10.1111/j.1460-9568.2007.05514.x.

Reyes-Haro, D., J. Müller, M. Boresch, T. Pivneva, B. Benedetti, A. Scheller, Ch. Nolte, and H. Kettenmann. 2010. "Neuron-Astrocyte Interactions in the Medial Nucleus of the Trapezoid Body." *The Journal of General Physiology* 135 (6): 583–94. doi:10.1085/jgp.200910354.

Rodríguez-Arellano, J. J., V. Parpura, R. Zorec, and A. Verkhratsky. 2016. "Astrocytes in Physiological Aging and Alzheimer's Disease." *Neuroscience* 323 (January). IBRO: 170–82. doi:10.1016/j.neuroscience.2015.01.007.

Roitbak, T., and E. Syková. 1999. "Diffusion Barriers Evoked in the Rat Cortex by Reactive Astrogliosis." *Glia* 28 (1): 40–48. doi:10.1002/(SICI)1098-1136(199910)28:1<40::AID-GLIA5>3.0.CO;2-6.

Sayed, R., W. Mubarak, A. Ohtsuka, T. Taguchi, and T. Murakami. 2002. "Histochemical Study of Perineuronal Nets in the Retrosplenial Cortex of Adult Rats." *Annals of Anatomy* 184 (4): 333–39. doi:10.1016/S0940-9602(02)80048-6.

Shellswell, G. B., D. J. Restall, V. C. Duance, and A. J. Bailey. 1979. “Identification and Differential Distribution of Collagen Types in the.” *North-Holland Biomedical Press* 106 (2): 305–8.

Sonntag, M., M. Blosa, S. Schmidt, R. Rübsamen, and M. Morawski. 2015. “Perineuronal Nets in the Auditory System.” *Hearing Research* 329. Elsevier B.V: 21–32. doi:10.1016/j.heares.2014.12.012.

Sotak, Ch. H. 2004. “Nuclear Magnetic Resonance (NMR) Measurement of the Apparent Diffusion Coefficient (ADC) of Tissue Water and Its Relationship to Cell Volume Changes in Pathological States.” *Neurochemistry International* 45 (4): 569–82. doi:10.1016/j.neuint.2003.11.010.

Spicer, A. P., A. Joo, and R. A. Bowling. 2003. “A Hyaluronan Binding Link Protein Gene Family Whose Members Are Physically Linked Adjacent to Chrondroitin Sulfate Proteoglycan Core Protein Genes.” *Journal of Biological Chemistry* 278 (23): 21083–91. doi:10.1074/jbc.M213100200.

Steele, M. L., and S. R. Robinson. 2012. “Reactive Astrocytes Give Neurons Less Support: Implications for Alzheimer’s Disease.” *Neurobiology of Aging* 33 (2). Elsevier Inc.: 423.e1-13. doi:10.1016/j.neurobiolaging.2010.09.018.

Suttkus, A., S. Rohn, C. Jäger, T. Arendt, and M. Morawski. 2012. “Neuroprotection against Iron-Induced Cell Death by Perineuronal Nets - an in Vivo Analysis of Oxidative Stress.” *American Journal of Neurodegenerative Disease* 1 (2): 122–29. http://www.pubmedcentral.nih.gov/articlerender.fcgi?artid=3560462&tool=pmcentrez&rendertype=abstract.

Svoboda, J., and E. Syková. 1991. “Extracellular Space Volume Changes in the Rat Spinal Cord Produced by Nerve Stimulation and Peripheral Injury.” *Brain Research* 560 (1–2): 216–24. http://eutils.ncbi.nlm.nih.gov/entrez/eutils/elink.fcgi?dbfrom=pubmed&id=1760728&retmode=ref&cmd=prlinks%5Cnpapers3://publication/uuid/0D30E19C-A5B7-4C6F-BE3C-45F3DA826A5D.

Syková, E., T. Mazel, R. U. Hasenöhrl, A. R. Harvey, Z. Šimonová, W. H. A. M. Mulders, and J. P. Huston. 2002. “Learning Deficits in Aged Rats Related to Decrease in Extracellular Volume and Loss of Diffusion Anisotropy in Hippocampus.” *Hippocampus* 12 (2): 269–79. doi:10.1002/hipo.1101.

Syková, E., T. Mazel, and Z. Šimonová. 1998. “Diffusion Constraints and Neuron-Glia Interaction during Aging.” *Experimental Gerontology* 33 (7–8): 837–51. doi:10.1016/S0531-5565(98)00038-2.

Syková, E., and Ch. Nicholson. 2008. “Diffusion in Brain Extracellular Space.” *Physiological Reviews* 88 (4): 1277–1340. doi:10.1152/physrev.00027.2007.Diffusion.

Syková, E., J. Svoboda, J. Polák, and A. Chvátal. 1994. “Extracellular Volume Fraction and Diffusion Characteristics during Progressive Ischemia and Terminal Anoxia in the Spinal Cord of the Rat.” *Journal of Cerebral Blood Flow and Metabolism* 14 (2): 301–11. doi:10.1038/jcbfm.1994.37.

Syková, E., and L. Vargová. 2008. “Extrasynaptic Transmission and the Diffusion Parameters of the Extracellular Space.” *Neurochemistry International* 52 (1–2): 5–13. doi:10.1016/j.neuint.2007.04.007.

Syková, E., L. Vargová, S. Kubinová, P. Jendelová, and A. Chvátal. 2003. “The Relationship between Changes in Intrinsic Optical Signals and Cell Swelling in Rat Spinal Cord

Slices." *NeuroImage* 18 (2): 214–30. doi:S1053811902000149 [pii].
Syková, E., L. Vargová, S. Prokopová, and Z. Šimonová. 1998. "Glial Swelling and Astrogliosis Produce Diffusion Barriers in the Rat Spinal Cord." *Glia* 25 (1): 56–70. doi:10.1002/(SICI)1098-1136(19990101)25:1<56::AID-GLIA6>3.0.CO;2-4.
Syková, E., I. Voříšek, T. Mazel, T. Antonova, and M. Schachner. 2005. "Reduced Extracellular Space in the Brain of Tenascin-R- and HNK-1-Sulphotransferase Deficient Mice." *European Journal of Neuroscience* 22 (8): 1873–80. doi:10.1111/j.1460-9568.2005.04375.x.
Taipale, J., and J. Keski-Oja. 1997. "Growth Factors in the Extracellular Matrix." *FASEB Journal: Official Publication of the Federation of American Societies for Experimental Biology* 11 (1): 51–59. http://www.ncbi.nlm.nih.gov/pubmed/9034166.
Takahashi-Iwanaga, H., T. Murakami, and K. Abe. 1998. "Three-Dimensional Microanatomy of Perineuronal Proteoglycan Nets Enveloping Motor Neurons in the Rat Spinal Cord." *Journal of Neurocytology* 27 (11): 817–27. doi:10.1023/A:1006955414939.
Theocharis, A. D., S. S. Skandalis, Ch. Gialeli, and N. K. Karamanos. 2015. "Extracellular Matrix Structure." *Advanced Drug Delivery Reviews* 97. Elsevier B.V.: 4–27. doi:10.1016/j.addr.2015.11.001.
Thorne, R. G., and Ch. Nicholson. 2006. "In Vivo Diffusion Analysis with Quantum Dots and Dextrans Predicts the Width of Brain Extracellular Space." *Proceedings of the National Academy of Sciences of the United States of America* 103 (14): 5567–72. doi:10.1073/pnas.0509425103.
Treherne, J. E., P. K. Schofield, and N. J. Lane. 1982. "Physiological and Ultrastructural Evidence for an Extracellular Anion Matrix in the Central Nervous System of an Insect (Periplaneta Americana)." *Brain Research* 247 (2): 255–67.
Van Harreveld, A., N. Dafny, and F. I. Khattab. 1971. "Effects of Calcium on the Electrical Resistance and the Extracellular Space of Cerebral Cortex." *Experimental Neurology* 31 (3): 358–67. http://www.sciencedirect.com/science/article/pii/001448867190238X.
Vargová, L., and E. Syková. 2008. "Extracellular Space Diffusion and Extrasynaptic Transmission." *Physiological Research* supplement: 89–99.
———. 2014. "Astrocytes and Extracellular Matrix in Extrasynaptic Volume Transmission." *Philosophical Transactions of the Royal Society of London. Series B, Biological Sciences* 369 (1654): 20130608. doi:10.1098/rstb.2013.0608.
Vo, T., D. Carulli, E. M. E. Ehlert, J. C. F. Kwok, G. Dick, V. Mecollari, E. B. Moloney, et al. 2013. "The Chemorepulsive Axon Guidance Protein semaphorin3A Is a Constituent of Perineuronal Nets in the Adult Rodent Brain." *Molecular and Cellular Neuroscience* 56. Elsevier Inc.: 186–200. doi:10.1016/j.mcn.2013.04.009.
Voříšek, I., M. Hájek, J. Tintěra, K. Nicolay, and Eva Syková. 2002. "Water ADC, Extracellular Space Volume, and Tortuosity in the Rat Cortex after Traumatic Injury." *Magnetic Resonance in Medicine* 48 (6): 994–1003. doi:10.1002/mrm.10305.
Voříšek, I., and E. Syková. 1997a. "Evolution of Anisotropic Diffusion in the Developing Rat Corpus Callosum." *Journal of Neurophysiology* 78 (2): 912–19.
———. 1997b. "Ischemia-Induced Changes in the Extracellular Space Diffusion Parameters, K+, and pH in the Developing Rat Cortex and Corpus Callosum." *Journal of Cerebral Blood Flow and Metabolism* 17 (2): 191–203. doi:10.1097/00004647-199702000-00009.

Vreugdenhil, M. 2002. “Parvalbumin-Deficiency Facilitates Repetitive IPSCs and Gamma Oscillations in the Hippocampus.” *Journal of Neurophysiology* 89 (3): 1414–22. doi:10.1152/jn.00576.2002.

Weber, P., U. Bartsch, M. N. Rasband, R. Czaniera, Y. Lang, H. Bluethmann, R. U. Margolis, et al. 1999. “Mice Deficient for Tenascin-R Display Alterations of the Extracellular Matrix and Decreased Axonal Conduction Velocities in the CNS.” *The Journal of Neuroscience : The Official Journal of the Society for Neuroscience* 19 (11): 4245–62.

Wegner, F., W. Härtig, A. Bringmann, J. Grosche, K. Wohlfarth, W. Zuschratter, and G. Brückner. 2003. “Diffuse Perineuronal Nets and Modified Pyramidal Cells Immunoreactive for Glutamate and the GABAA Receptor α1 Subunit Form a Unique Entity in Rat Cerebral Cortex.” *Experimental Neurology* 184 (2): 705–14. doi:10.1016/S0014-4886(03)00313-3.

Weiser, M., E. Bueno, C. Sekirnjak, M. E. Martone, H. Baker, D. Hillman, S. Chen, W. Thornhill, M. Ellisman, and B. Rudy. 1995. “The Potassium Channel Subunit KV3.1b Is Localized to Somatic and Axonal Membranes of Specific Populations of CNS Neurons.” *The Journal of Neuroscience : The Official Journal of the Society for Neuroscience* 15 (6): 4298–4314. http://www.ncbi.nlm.nih.gov/pubmed/7790912.

Xiao, F., Ch. Nicholson, J. Hrabe, and S. Hrabetová. 2008. “Diffusion of Flexible Random-Coil Dextran Polymers Measured in Anisotropic Brain Extracellular Space by Integrative Optical Imaging.” *Biophysical Journal* 95 (3): 1382–92. doi:10.1529/biophysj.107.124743.

Yamada, J., and S. Jinno. 2013. “Spatio-Temporal Differences in Perineuronal Net Expression in the Mouse Hippocampus, with Reference to Parvalbumin.” *Neuroscience* 253. IBRO: 368–79. doi:10.1016/j.neuroscience.2013.08.061.

Yang, S., M. Cacquevel, L. M. Saksida, T. J. Bussey, B. L. Schneider, P. Aebischer, R. Melani, T. Pizzorusso, J. W. Fawcett, and M. G. Spillantini. 2015. “Perineuronal Net Digestion with Chondroitinase Restores Memory in Mice with Tau Pathology.” *Experimental Neurology* 265. Elsevier B.V.: 48–58. doi:10.1016/j.expneurol.2014.11.013.

Ye, Q., and Q. L. Miao. 2013. “Experience-Dependent Development of Perineuronal Nets and Chondroitin Sulfate Proteoglycan Receptors in Mouse Visual Cortex.” *Matrix Biology* 32 (6). International Society of Matrix Biology: 352–63. doi:10.1016/j.matbio.2013.04.001.

Yong, V. W., C. Power, P. Forsyth, and D. R. Edwards. 2001. “Metalloproteinases in Biology and Pathology of the Nervous System.” *Nature Reviews. Neuroscience* 2 (7): 502–11. doi:10.1038/35081571.

Zámečník, J., A. Homola, M. Cicanic, K. Kuncova, P. Marusic, P. Krsek, E. Sykova, and L. Vargova. 2012. “The Extracellular Matrix and Diffusion Barriers in Focal Cortical Dysplasias.” *European Journal of Neuroscience* 36 (1): 2017–24. doi:10.1111/j.1460-9568.2012.08107.x.

Zámečník, J., L. Vargová, a. Homola, R. Kodet, and E. Syková. 2004. “Extracellular Matrix Glycoproteins and Diffusion Barriers in Human Astrocytic Tumours.” *Neuropathology and Applied Neurobiology* 30 (4): 338–50. doi:10.1046/j.0305-1846.2003.00541.x.

Zhou, X., C. Brakebusch, H. Matthies, T. Oohashi, E. Hirsch, M. Moser, M. Krug, et al. 2001. “Neurocan Is Dispensable for Brain Development.” *Molecular and Cellular*

Biology 21 (17): 5970–78. doi:10.1128/MCB.21.17.5970.
Zoli, M., A. Jansson, E. Syková, L. F. Agnati, and K. Fuxe. 1999. “Volume Transmission in the CNS and Its Relevance for Neuropsychopharmacology.” *Trends in Pharmacological Sciences* 20 (4): 142–50. doi:10.1016/S0165-6147(99)01343-7.